

Reconfigurable Intelligent Surface-Assisted Cell-Free Massive MIMO Systems Over Spatially-Correlated Channels

Trinh Van Chien, *Member, IEEE*, Hien Quoc Ngo, *Senior Member, IEEE*, Symeon Chatzinotas, *Senior Member, IEEE*, Marco Di Renzo, *Fellow, IEEE*, and Björn Ottersten, *Fellow, IEEE*

Abstract

Cell-Free Massive multiple-input multiple-output (MIMO) and reconfigurable intelligent surface (RIS) are two promising technologies for application to beyond-5G networks. This paper considers Cell-Free Massive MIMO systems with the assistance of an RIS for enhancing the system performance under the presence of spatial correlation among the scattering elements of the RIS. Distributed maximum-ratio processing is considered at the access points (APs). We introduce an *aggregated channel* estimation approach that provides sufficient information for data processing with the main benefit of reducing the overhead required for channel estimation. The considered system is studied by using asymptotic analysis which lets the number of APs and/or the number of RIS elements grow large. A lower bound for the channel capacity is obtained for a finite number of APs and scattering elements of the RIS, and closed-form expressions for the uplink and downlink ergodic net throughput are formulated in terms of only the channel statistics. Based on the obtained analytical frameworks, we unveil the impact of channel correlation, the number of RIS elements, and the pilot contamination on the net throughput of each user. In addition, a simple control scheme for controlling the configuration of the scattering elements of the RIS is proposed, which is shown to increase the channel estimation quality, and, hence, the system performance. Numerical results demonstrate the effectiveness of our system design and performance analysis. In particular, the performance benefits of using RISs in Cell-Free Massive MIMO systems are confirmed, especially if the direct links between the APs and the users are of insufficient quality with a high probability.

Index Terms

T. V. Chien, S. Chatzinotas, B. Ottersten are with the Interdisciplinary Centre for Security, Reliability and Trust (SnT), University of Luxembourg, L-1855 Luxembourg, Luxembourg (email: vanchien.trinh@uni.lu, symeon.chatzinotas@uni.lu, and bjorn.ottersten@uni.lu). H. Q. Ngo is with the School of Electronics, Electrical Engineering and Computer Science, Queen's University Belfast, Belfast BT7 1NN, United Kingdom (email: hien.ngo@qub.ac.uk). M. Di Renzo is with Université Paris-Saclay, CNRS, CentraleSupélec, Laboratoire des Signaux et Systèmes, 91192 Gif-sur-Yvette, France (email: marco.di-renzo@universite-paris-saclay.fr). Parts of this paper will be submitted to IEEE GLOBECOM 2021 [1].

Cell-free Massive MIMO, reconfigurable intelligent surface, maximum ratio processing, ergodic net throughput.

I. INTRODUCTION

In the last few decades, we have witnessed an exponential growth of the demand for wireless communication systems that provide reliable communications and ensure ubiquitous coverage, high spectral efficiency and low latency [2]. To meet these requirements, several new technologies have been incorporated in 5G communication standards, which include Massive multiple-input multiple-output (MIMO) [3], millimeter-wave communications [4], and network densification [5]. Among them, Massive MIMO has gained significant attention since it can offer a good service to many users in the network. Moreover, the net throughput offered by a Massive MIMO system is close to the Shannon capacity, in many scenarios, by only employing simple linear processing techniques, such as maximum ratio (MR) or zero forcing (ZF) processing. Since the net throughput can be computed in a closed-form expression that only depends on the channel statistics, the optimization solutions are applicable for a long period of time [6]. The colocated Massive MIMO architecture has the advantage of low backhaul requirements since the base station antennas are installed in a compact array. Conventional cellular networks, however, are impaired by intercell interference. In particular, the users at the cell boundaries are impaired by high intracell interference and path loss, and hence, they may experience insufficient performance. More advanced signal processing methods are necessary to overcome the inherent intercell interference that characterizes conventional cellular network deployments.

Cell-Free Massive MIMO has recently been introduced to reduce the intercell interference of colocated Massive MIMO architectures. Cell-Free Massive MIMO is a network deployment where a large number of access points (APs) are located in a given coverage area to serve a small number of users [7], [8]. All APs collaborate with each other via a backhaul network and serve all the users in the absence of cell boundaries. The system performance is enhanced in Cell-Free Massive MIMO systems because they inherit the benefits of the distributed MIMO and network MIMO architectures, but the users are also close to the APs. When each AP is equipped with a single antenna, MR processing results in a good net throughput for every user, while ensuring a low computational complexity and offering a distributed implementation that is convenient for scalability purposes [9]. However, Cell-Free Massive MIMO cannot guarantee a good quality of service under harsh propagation conditions, such as in the presence of poor scattering environments or high attenuation due to large obstacles.

Reconfigurable intelligent surface (RIS) is an emerging technology that is capable of shaping the radio waves at the electromagnetic level without applying digital signal processing methods and without requiring power amplifiers [10]–[12]. Each element of the RIS scatters (e.g., reflects) the incident signal without using radio frequency chains and power amplification [13]. Integrating an

RIS into wireless networks introduces digitally controllable links that scale up with the number of scattering elements of the RIS, whose estimation is, however, challenged by the lack of digital signal processing units at the RIS [14]–[18]. For simplicity, the main attention has so far been concentrated on designing the phase shifts with perfect channel state information (CSI) [14], [19] and the references therein. In [18], the authors have recently discussed the fundamental issues of performing channel estimation in RIS-assisted wireless systems. The impact of channel estimation overhead and reporting on the spectral efficiency, energy efficiency, and their tradeoff has recently been investigated in [15]. In [14] and [16], to reduce the impact of channel estimation overhead, the authors have investigated the design of RIS-assisted communications in the presence of statistical CSI. As far as the integration of Cell-Free Massive MIMO and RIS is concerned, recent works have formulated and solved optimization problems with different communication objectives under the assumption of perfect (and instantaneous) CSI [20]–[24]. Recent results in the context of single-input single-output (SISO) and multi-user MIMO systems have, however, shown that designs for the phase shifts of the RIS elements that are based on statistical CSI may be of practical interest and provide good performance [16], [25]–[27].

In the depicted context, no prior work has analyzed the performance of RIS-assisted Cell-Free Massive MIMO systems in the presence of spatially-correlated channels. In this work, motivated by these considerations, we introduce an analytical framework for analyzing and optimizing the uplink and downlink transmission of RIS-assisted Cell-Free Massive MIMO systems under spatially correlated channels and in the presence of direct links subject to the presence of blockages. In particular, the main contributions made by this paper can be summarized as follows:

- We consider an RIS-assisted Cell-Free Massive MIMO under spatially correlated channels. All APs estimate the instantaneous channels in the uplink pilot training phase. We exploit a channel estimation scheme that estimates the aggregated channels including both the direct and indirect links, instead of every individual channel coefficient as in previous works [18], [22]. For generality, the pilot contamination is assumed to originate from an arbitrary pilot reuse pattern.
- We analytically show that, even by using a low complexity MR technique, the non-coherent interference, small-scale fading effects, and additive noise are averaged out when the number of APs and RIS elements increases. The received signal includes, hence, only the desired signal and the coherent interference. Besides, the indirect links become dominant if the number of phase shifts increases.
- We derive a closed-form expression of the net throughput for both the uplink and downlink data transmissions. The impact of the array gain, coherent joint transmission, channel estimation errors, pilot contamination, spatial correlation, and phase shifts of the RIS, which determine the system performance, are explicitly observable in the obtained analytical expressions.

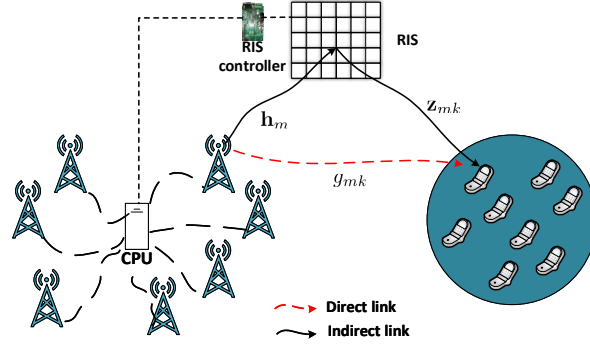


Fig. 1. An RIS-assisted Cell-Free Massive MIMO system where M APs collaborate with each other to serve K distant users.

- With the aid of numerical simulations, we verify the effectiveness of the proposed channel estimation scheme and the accuracy of the closed-form expressions of the net throughput. The obtained numerical results show that the use of RISs enhance the net throughput per user significantly, especially when the direct links are blocked with high probability.

The rest of this paper is organized as follows: Section II presents the system model, the channel model, and the channel estimation protocol. The uplink data transmission protocol and the asymptotic analysis by assuming a very large number of APs and phase shifts of the RIS are discussed in Section III. A similar analysis for the downlink data transmission is reported in Section IV. Finally, Section V illustrates several numerical results, while the main conclusions are drawn in Section VI.

Notation: Upper and lower bold letters are used to denote matrices and vectors, respectively. The identity matrix of size $N \times N$ is denoted by \mathbf{I}_N . The imaginary unit of a complex number is denoted by j with $\sqrt{j} = -1$. The superscripts $(\cdot)^*$, $(\cdot)^T$, and $(\cdot)^H$ denote the complex conjugate, transpose, and Hermitian transpose, respectively. $\mathbb{E}\{\cdot\}$ and $\text{Var}\{\cdot\}$ denote the expectation and variance of a random variable. The circularly symmetric Gaussian distribution is denoted by $\mathcal{CN}(\cdot, \cdot)$ and $\text{diag}(\mathbf{x})$ is the diagonal matrix whose main diagonal is given by \mathbf{x} . $\text{tr}(\cdot)$ is the trace operator. The Euclidean norm of vector \mathbf{x} is $\|\mathbf{x}\|$, and $\|\mathbf{X}\|$ is the spectral norm of matrix \mathbf{X} . Finally, $\text{mod}(\cdot, \cdot)$ is the modulus operation and $\lfloor \cdot \rfloor$ denotes the truncated argument.

II. SYSTEM MODEL, CHANNEL ESTIMATION, AND RIS PHASE SHIFT CONTROL

We consider an RIS-assisted Cell-Free Massive MIMO system, where M APs connected to a central processing unit (CPU) serve K users on the same time and frequency resource, as schematically illustrated in Fig. 1. All APs and users are equipped with a single antenna and they are randomly located in the coverage area. Since the considered users are far away from the APs, the communication is assisted by an RIS that comprises N scattering elements that can modify the phases of the incident

signals.¹ The matrix of phase shifts of the RIS is denoted by $\Phi = \text{diag}([e^{j\theta_1}, \dots, e^{j\theta_N}]^T)$, where $\theta_n \in [-\pi, \pi]$ is the phase shift applied by the n -th element of the RIS. The phase shifts are adjusted by a controller which exchanges information with the APs via a backhaul link (see Fig. 1). As a canonical form of Cell-Free Massive MIMO systems, we assume that the system operates in time-division duplexing (TDD) mode. Thus, we assume that channel reciprocity holds in the consisted system model.

A. Channel Model

We assume a quasi-static block fading model where the channels are static and frequency flat in each coherence interval comprising τ_c symbols. We assume that the APs have knowledge of only the channel statistics instead of the instantaneous channel realizations. Also, τ_p symbols ($\tau_p < \tau_c$) in each coherence interval are dedicated to the channel estimation and the remaining $(\tau_c - \tau_p)$ symbols are utilized for the uplink and downlink data transmissions.

The following notation is used: g_{mk} is the channel between the user k and the AP m , which is the direct link [10]; $\mathbf{h}_m \in \mathbb{C}^N$ is the channel between the AP m and the RIS; and $\mathbf{z}_{mk} \in \mathbb{C}^N$ is the channel between the RIS and the user k . Each pair of the cascaded channels \mathbf{h}_m and \mathbf{z}_{mk} results in an indirect link (virtual line-of-sight link), which enhances the communication reliability between the AP m and the user k [28]. The majority of existing works assume that the wireless channels undergo uncorrelated Rayleigh fading. In this paper, we consider a more realistic channel model by taking into account the spatial correlation among the scattering elements of the RIS, which is due to their sub-wavelength size, sub-wavelength inter-distance, and geometric layout. In an isotropic propagation environment, in particular, g_{mk} , \mathbf{h}_m , and \mathbf{z}_{mk} can be modeled as follows

$$g_{mk} \sim \mathcal{CN}(0, \beta_{mk}), \mathbf{h}_m \sim \mathcal{CN}(\mathbf{0}, \mathbf{R}_m), \mathbf{z}_{mk} \sim \mathcal{CN}(\mathbf{0}, \tilde{\mathbf{R}}_{mk}), \quad (1)$$

where β_{mk} is the large-scale fading coefficient; $\mathbf{R}_m \in \mathbb{C}^{N \times N}$ and $\tilde{\mathbf{R}}_{mk} \in \mathbb{C}^{N \times N}$ are the covariance matrices that characterize the spatial correlation among the channels of the RIS elements. The covariance matrices in (1) correspond to a general model, which can be further particularized for application to typical RIS designs and propagation environments. For example, a simple exponential model was used to describe the spatial correlation among the scattering elements of the RIS in [29]. Another recent model that is applicable to isotropic scattering with uniformly distributed multipath components in the half-space in front of the RIS was recently reported in [30], whose covariance matrices are

$$\mathbf{R}_m = \alpha_m d_H d_V \mathbf{R} \text{ and } \tilde{\mathbf{R}}_{mk} = \tilde{\alpha}_{mk} d_H d_V \mathbf{R}, \quad (2)$$

¹In general, there are also users that are close to the APs. However, we aim at improving the data rates of the users who are far away from the APs, and, hence, have very weak direct channels to the APs. The users near the APs are not considered.

where $\alpha_m, \tilde{\alpha}_{mk} \in \mathbb{C}$ are the large-scale channel coefficients. The matrices in (2) assume that the size of each element of the RIS is $d_H \times d_V$, with d_H being the horizontal width and d_V being the vertical height of each RIS element. In particular, the (m', n') -th element of the spatial correlation matrix $\mathbf{R} \in \mathbb{C}^{N \times N}$ in (2) is

$$[\mathbf{R}]_{m'n'} = \text{sinc}(2\|\mathbf{u}_{m'} - \mathbf{u}_{n'}\|/\lambda), \quad (3)$$

where λ is the wavelength and $\text{sinc}(x) = \sin(\pi x)/(\pi x)$ is the sinc function. The vector $\mathbf{u}_x, x \in \{m', n'\}$ is given by

$$\mathbf{u}_x = [0, \quad \text{mod}(x-1, N_H)d_H, \lfloor (x-1)/N_H \rfloor d_V]^T, \quad (4)$$

where N_H and N_V denote the total number of RIS elements in each row and column, respectively. The channel model in (1) is significantly distinct from related works since the small-scale fading and the spatial correlation matrices are included in both links of the virtual line-of-sight link that comprises the RIS. In [29], by contrast, the channels between the transmitters and the RIS are assumed to be deterministic, for analytical tractability.

B. Uplink Pilot Training Phase

The channels are independently estimated from the τ_p pilot sequences transmitted by the K users. All the users share the same τ_p pilot sequences. In particular, $\phi_k \in \mathbb{C}^{\tau_p}$ with $\|\phi_k\|^2 = 1$ is defined as the pilot sequence allocated to the user k . We denote by \mathcal{P}_k the set of indices of the users (including the user k) that share the same pilot sequence as the user k . The pilot sequences are assumed to be mutually orthogonal such that the pilot reuse pattern is

$$\phi_{k'}^H \phi_k = \begin{cases} 1, & \text{if } k' \in \mathcal{P}_k, \\ 0, & \text{if } k' \notin \mathcal{P}_k. \end{cases} \quad (5)$$

During the pilot training phase, all the K users transmit the pilot sequences to the M APs simultaneously. In particular, the user k transmits the pilot sequence $\sqrt{\tau_p}\phi_k$. The received training signal at the AP m , $\mathbf{y}_{pm} \in \mathbb{C}^{\tau_p}$, can be written as

$$\mathbf{y}_{pm} = \sum_{k=1}^K \sqrt{p\tau_p} g_{mk} \phi_k + \sum_{k=1}^K \sqrt{p\tau_p} \mathbf{h}_m^H \Phi \mathbf{z}_{mk} \phi_k + \mathbf{w}_{pm}, \quad (6)$$

where p is the normalized signal-to-noise ratio (SNR) of each pilot symbol, and $\mathbf{w}_{pm} \in \mathbb{C}^{\tau_p}$ is the additive noise at the AP m , which is distributed as $\mathbf{w}_{pm} \sim \mathcal{CN}(\mathbf{0}, \mathbf{I}_{\tau_p})$. In order for the AP m to estimate the desired channels from the user k , the received training signal in (6) is projected on ϕ_k^H as

$$y_{pmk} = \phi_k^H \mathbf{y}_{pm} = \sqrt{p\tau_p} (g_{mk} + \mathbf{h}_m^H \Phi \mathbf{z}_{mk}) + \sum_{k' \in \mathcal{P}_k \setminus \{k\}} \sqrt{p\tau_p} (g_{mk'} + \mathbf{h}_m^H \Phi \mathbf{z}_{mk'}) + w_{pmk}, \quad (7)$$

where $w_{pmk} = \phi_k^H \mathbf{w}_{pm} \sim \mathcal{CN}(0, 1)$. We emphasize that the co-existence of direct and indirect channels due to the presence of the RIS results in a complicated channel estimation process. In particular, the cascaded channel in (7) results in a nontrivial procedure to apply the minimum mean-square error (MMSE) estimation method, as reported in previous works, for processing the projected signals [7], [8]. Based on specific signal structure in (7), we denote the channel between the AP m and the user k through the RIS as

$$u_{mk} = g_{mk} + \mathbf{h}_m^H \Phi \mathbf{z}_{mk}, \quad (8)$$

which is referred to as the *aggregated channel* that comprises the direct and indirect link between the user k and the AP m . By capitalizing on the definition of the aggregated channel in (8), the required channels can be estimated in an effective manner even in the presence of the RIS. In particular, the aggregated channel in (8) is given by the product of weighted complex Gaussian and spatially correlated random variables, as given in (1). Despite the complex analytical form, the following lemma gives information on the statistics of the aggregated channel u_{mk} , $\forall m, k$.

Lemma 1. *The second and fourth moments of the aggregated channel u_{mk} can be formulated as follows*

$$\mathbb{E}\{|u_{mk}|^2\} = \beta_{mk} + \text{tr}(\Phi^H \mathbf{R}_m \Phi \tilde{\mathbf{R}}_{mk}), \quad (9)$$

$$\mathbb{E}\{|u_{mk}|^4\} = 2 \left(\beta_{mk} + \text{tr}(\Phi^H \mathbf{R}_m \Phi \tilde{\mathbf{R}}_{mk}) \right)^2 + 2 \text{tr} \left((\Phi^H \mathbf{R}_m \Phi \tilde{\mathbf{R}}_{mk})^2 \right). \quad (10)$$

Proof. See Appendix B. □

The moments in Lemma 1 are employed next for channel estimation and for analyzing the net throughput. We note, in addition, that the odd moments of u_{mk} , e.g., the first and third moments, are equal to zero. Conditioned on the phase shifts, we employ the linear MMSE method for estimating u_{mk} at the AP. In spite of the complex structure of the RIS-assisted cascaded channel, Lemma 2 provides analytical expressions of the estimated channels.

Lemma 2. *By assuming that the AP m employs the linear MMSE estimation method based on the observation in (7), the estimate of the aggregate channel u_{mk} can be formulated as*

$$\hat{u}_{mk} = (\mathbb{E}\{y_{pmk}^* u_{mk}\} y_{pmk}) / \mathbb{E}\{|y_{pmk}|^2\} = c_{mk} y_{pmk}, \quad (11)$$

where $c_{mk} = \mathbb{E}\{y_{pmk}^* u_{mk}\} / \mathbb{E}\{|y_{pmk}|^2\}$ has the following closed-form expression

$$c_{mk} = \frac{\sqrt{p\tau_p} (\beta_{mk} + \text{tr}(\Phi^H \mathbf{R}_m \Phi \tilde{\mathbf{R}}_{mk}))}{p\tau_p \sum_{k' \in \mathcal{P}_k} (\beta_{mk'} + \text{tr}(\Phi^H \mathbf{R}_m \Phi \tilde{\mathbf{R}}_{mk'})) + 1}. \quad (12)$$

The estimated channel in (11) has zero mean and variance γ_{mk} equal to

$$\gamma_{mk} = \mathbb{E}\{|\hat{u}_{mk}|^2\} = \sqrt{p\tau_p} (\beta_{mk} + \text{tr}(\Phi^H \mathbf{R}_m \Phi \tilde{\mathbf{R}}_{mk})) c_{mk}. \quad (13)$$

Also, the channel estimation error $e_{mk} = u_{mk} - \hat{u}_{mk}$ and the channel estimate \hat{u}_{mk} are uncorrelated. Furthermore, the channel estimation error has zero mean and variance equal to

$$\mathbb{E}\{|e_{mk}|^2\} = \beta_{mk} + \text{tr}(\Phi^H \mathbf{R}_m \Phi \tilde{\mathbf{R}}_{mk}) - \gamma_{mk}. \quad (14)$$

Proof. It is similar to the proof in [31], and is obtained by applying similar analytical steps to the received signal in (7) and by taking into account the structure of the RIS-assisted cascaded channel and the spatial correlation matrices in (1). \square

Lemma 2 shows that, by assuming Φ fixed, the aggregated channel in (8) can be estimated without increasing the pilot training overhead, as compared to a conventional Cell-Free Massive MIMO system. The obtained channel estimate in (11) unveils the relation $\hat{u}_{mk'} = \frac{c_{mk'}}{c_{mk}} \hat{u}_{mk}$ if the user k' uses the same pilot sequence as the user k . This implies that, because of pilot contamination, it may be difficult to distinguish the signals of these two users. In that regard it is worth noting that, to get rid of pilot contamination, one can assign mutually orthogonal pilot signals to all the users in the network (if the coherence time is long enough so that $\tau_p \geq K$). Under mutually orthogonal pilot sequences, c_{mk} and γ_{mk} simplify to c_{mk}^o and γ_{mk}^o , respectively, as follows

$$c_{mk}^o = \frac{\sqrt{p\tau_p}(\beta_{mk} + \text{tr}(\Phi^H \mathbf{R}_m \Phi \tilde{\mathbf{R}}_{mk}))}{p\tau_p(\beta_{mk} + \text{tr}(\Phi^H \mathbf{R}_m \Phi \tilde{\mathbf{R}}_{mk})) + 1}, \quad \gamma_{mk}^o = \sqrt{p\tau_p}(\beta_{mk} + \text{tr}(\Phi^H \mathbf{R}_m \Phi \tilde{\mathbf{R}}_{mk}))c_{mk}^o. \quad (15)$$

This implies that, in the absence of pilot contamination, we have $\gamma_{mk}^o \rightarrow \beta_{mk} + \text{tr}(\Phi^H \mathbf{R}_m \Phi \tilde{\mathbf{R}}_{mk})$ as $\tau_p \rightarrow \infty$, i.e., the variance of the channel estimation error in (13) is equal to zero. The channel estimates given in Lemma 2 can be applied to an arbitrary set of phase shifts and covariance matrices. In the following, the analytical expression of the channel estimates in Lemma 2 are employed for signal detection in the uplink and for beamforming in the downlink. They are used also to optimize the phase shifts of the RIS in order to minimize the channel estimation error and to evaluate the corresponding ergodic net throughput.

C. RIS Phase Shift Control and Optimization

Channel estimation is a critical aspect in Cell-Free Massive MIMO. As discussed in previous text, in many scenarios, non-orthogonal pilots have to be used. This causes pilot contamination, which may reduce the system performance significantly. In this section, we design an RIS-assisted phase shift control scheme that is aimed to improve the quality of channel estimation. To this end, we introduce the normalized mean square error (NMSE) of the channel estimate of the user k at the AP m as follows

$$\text{NMSE}_{mk} = \frac{\mathbb{E}\{|e_{mk}|^2\}}{\mathbb{E}\{|u_{mk}|^2\}} = 1 - \frac{p\tau_p(\beta_{mk} + \text{tr}(\Phi^H \mathbf{R}_m \Phi \tilde{\mathbf{R}}_{mk}))}{p\tau_p \sum_{k' \in \mathcal{P}_k} (\beta_{mk'} + \text{tr}(\Phi^H \mathbf{R}_m \Phi \tilde{\mathbf{R}}_{mk'})) + 1}, \quad (16)$$

where the last equality is obtained from (9) and (14). We propose to optimize the phase shift matrix Φ of the RIS so as to minimize the total NMSE obtained from all the users and all the APs as follows

$$\begin{aligned} & \underset{\{\theta_n\}}{\text{minimize}} && \sum_{m=1}^M \sum_{k=1}^K \text{NMSE}_{mk} \\ & \text{subject to} && -\pi \leq \theta_n \leq \pi, \forall n. \end{aligned} \quad (17)$$

We emphasize that the optimal phase shifts solution to problem (17) is obtained by exploiting the statistical CSI that include the large-scale fading coefficients and the covariance matrices. Problem (17) is a fractional program, whose globally-optimal solution is not simple to be obtained for an RIS with a large number of independently tunable elements. Nonetheless, in the special network setup where the direct links from the APs to the users are weak enough to be negligible with respect to the RIS-assisted links, the optimal solution to problem (17) is available in a closed-form expression as summarized in Corollary 1.

Corollary 1. *If the direct links are weak enough to be negligible and the RIS-assisted channels are spatially correlated as formulated in (2), the optimal maximizer of the optimization problem in (17) is $\theta_1 = \dots = \theta_N$, i.e., the equal phase shift design is optimal.*

Proof. See Appendix C. □

Corollary 1 provides a simple but effective option to design the phase shifts of the RIS while ensuring the optimal estimation of the aggregated channels according to the sum-NMSE minimization criterion, provided that the direct link are completely blocked and the spatial correlation model in (2) holds true. Therefore, an efficient channel estimation protocol can be designed even in the presence of an RIS with a large number of scattering elements. The numerical results in Section V show that the phase shift design in Corollary 1 offers good gains in terms of net throughput even if the direct links are not negligible.

Remark 1. *The proposed optimization method of the phase shifts of the RIS is based on the minimization of the sum-NMSE, and it is, therefore, based on improving the channel estimation quality. This is a critical objective in Massive MIMO systems, since improving the accuracy of channel estimation results in a noticeable enhancement of the uplink and downlink net throughput [32], [33]. Another option would be to optimize the phase shifts of the RIS based on the maximization of the uplink or downlink ergodic net throughput. The solution of the corresponding optimization problem is, however, challenging and depends on whether the uplink or the downlink transmission phases are considered. Due to space limitations, therefore, we postpone this latter criterion for optimizing the phase shifts of the RIS to a future research work.*

III. UPLINK DATA TRANSMISSION AND PERFORMANCE ANALYSIS WITH MR COMBINING

In this section, we first introduce a procedure to detect the uplink transmitted signals by capitalizing on the channel estimation method introduced in the previous section. Then, we derive an asymptotic closed-form expression of the ergodic net throughput.

A. Uplink Data Transmission Phase

In the uplink, all the K users transmit their data to the M APs simultaneously. Specifically, the user k transmits a modulated symbol s_k with $\mathbb{E}\{|s_k|^2\} = 1$. This symbol is weighted by a power control factor $\sqrt{\eta_k}$, $0 \leq \eta_k \leq 1$. Then, the received baseband signal, $y_{um} \in \mathbb{C}$, at the AP m is

$$y_{um} = \sqrt{\rho_u} \sum_{k=1}^K \sqrt{\eta_k} (g_{mk} + \mathbf{h}_m^H \Phi \mathbf{z}_{mk}) s_k + w_{um} = \sqrt{\rho_u} \sum_{k=1}^K \sqrt{\eta_k} u_{mk} s_k + w_{um}, \quad (18)$$

where ρ_u is the normalized uplink SNR of each data symbol and w_{um} is the normalized additive noise with $w_{um} \sim \mathcal{CN}(0, 1)$. For data detection, the MR combining method is used at the CPU, i.e., $\hat{u}_{mk}, \forall m, k$, in (11) is employed to detect the data transmitted by the user k . In mathematical terms, the corresponding decision statistic is

$$r_{uk} = \sum_{m=1}^M \hat{u}_{mk}^* y_{um} = \sqrt{\rho_u} \sum_{m=1}^M \sum_{k'=1}^K \sqrt{\eta_{k'}} \hat{u}_{mk}^* u_{mk'} s_{k'} + \sum_{m=1}^M \hat{u}_{mk}^* w_{um}. \quad (19)$$

Based on the observation r_{uk} , the uplink ergodic net throughput of the user k is analyzed in the next subsection.

B. Asymptotic Analysis of the Uplink Received Signal

In the considered system model, the number of APs, M , and the number of tunable elements of the RIS, N , can be large. Therefore, we analyze the performance of two case studies: (i) N is fixed and M is large; and (ii) both N and M are large but their ratio is fixed. The asymptotic analysis is conditioned upon a given setup of the CSI, which includes the large-scale fading coefficients, the covariance matrices, and the power utilized for pilot and data transmissions. To this end, the uplink weighted signal in (19) is split into three terms based on the pilot reuse set \mathcal{P}_k , as follows

$$r_{uk} = \underbrace{\sqrt{\rho_u} \sum_{k' \in \mathcal{P}_k} \sum_{m=1}^M \sqrt{\eta_{k'}} \hat{u}_{mk}^* u_{mk'} s_{k'}}_{\mathcal{T}_{k1}} + \underbrace{\sqrt{\rho_u} \sum_{k' \notin \mathcal{P}_k} \sum_{m=1}^M \sqrt{\eta_{k'}} \hat{u}_{mk}^* u_{mk'} s_{k'}}_{\mathcal{T}_{k2}} + \underbrace{\sum_{m=1}^M \hat{u}_{mk}^* w_{um}}_{\mathcal{T}_{k3}}, \quad (20)$$

where \mathcal{T}_{k1} accounts for the signals received from all the users in \mathcal{P}_k , and \mathcal{T}_{k2} accounts for the mutual interference from the users that are assigned orthogonal pilot sequences. The impact of the additive

noise obtained after applying MR combining is given by \mathcal{T}_{k3} . From (7), (8), and (11), we obtain the following identity

$$\begin{aligned} \sum_{m=1}^M \sqrt{\eta_{k'}} \hat{u}_{mk}^* u_{mk'} &= \sum_{m=1}^M \sqrt{\eta_{k'}} c_{mk} u_{mk'} \left(\sum_{k'' \in \mathcal{P}_k} \sqrt{p} \tau_p u_{mk''}^* + w_{pmk}^* \right) \\ &= \sum_{m=1}^M \sqrt{\eta_{k'} p \tau_p} c_{mk} |u_{mk'}|^2 + \sum_{k'' \in \mathcal{P}_k \setminus \{k'\}} \sum_{m=1}^M \sqrt{\eta_{k'} p \tau_p} c_{mk} u_{mk'} u_{mk''}^* + \sum_{m=1}^M \sqrt{\eta_{k'}} c_{mk} u_{mk'} w_{pmk}^*. \end{aligned} \quad (21)$$

1) *Case I:* N is fixed and M is large, i.e., $M \rightarrow \infty$. In this case, we divide both sides of (21) by M and exploits Tchebyshev's theorem [34]² and (9) to obtain

$$\frac{1}{M} \sum_{m=1}^M \sqrt{\eta_{k'}} \hat{u}_{mk}^* u_{mk'} \xrightarrow{P} \frac{1}{M} \sum_{m=1}^M \sqrt{\eta_{k'} p \tau_p} c_{mk} (\beta_{mk'} + \text{tr}(\Phi^H \mathbf{R}_m \Phi \tilde{\mathbf{R}}_{mk'})), \quad (22)$$

where \xrightarrow{P} denotes the convergence in probability.³ Note that the second and third terms in (21) converge to zero. By inserting (22) into the decision variable in (20), we obtain the following deterministic value

$$\frac{1}{M} r_{uk} \xrightarrow{P} \frac{1}{M} \sum_{k' \in \mathcal{P}_k} \sum_{m=1}^M \sqrt{\eta_{k'} p \tau_p} c_{mk} (\beta_{mk'} + \text{tr}(\Phi^H \mathbf{R}_m \Phi \tilde{\mathbf{R}}_{mk'})) s_{k'}, \quad (23)$$

because $\mathcal{T}_{k2}/M \rightarrow 0$ and $\mathcal{T}_{k3}/M \rightarrow 0$ as $M \rightarrow \infty$. The result in (23) unveils that, for a fixed N , the channels become asymptotically orthogonal. In particular, the small-scale fading, the non-coherent interference, and the additive noise vanish. The only residual impairment is the pilot contamination caused by the users that employ the same pilot sequence. This result is the evidence that, due to pilot contamination, the system performance cannot be improved by adding more APs if MR combining is used. The contributions of both the direct and RIS-assisted indirect channels appear explicitly in (23) through the terms $\beta_{mk'}$ and $\text{tr}(\Phi^H \mathbf{R}_m \Phi \tilde{\mathbf{R}}_{mk'})$, respectively.

2) *Case II:* Both N and M are large, i.e., $N \rightarrow \infty$ and $M \rightarrow \infty$. To analyze this case study, we need some assumptions on the covariance matrices \mathbf{R}_m and $\tilde{\mathbf{R}}_{mk}$, as summarized as follows.

Assumption 1. For $m = 1, \dots, M$ and $k = 1, \dots, K$, the covariance matrices \mathbf{R}_m and $\tilde{\mathbf{R}}_{mk}$ are assumed to fulfill the following properties

$$\limsup_N \|\mathbf{R}_m\|_2 < \infty, \liminf_N \frac{1}{N} \text{tr}(\mathbf{R}_m) > 0, \quad (24)$$

$$\limsup_N \|\tilde{\mathbf{R}}_{mk}\|_2 < \infty, \liminf_N \frac{1}{N} \text{tr}(\tilde{\mathbf{R}}_{mk}) > 0. \quad (25)$$

²Let X_1, \dots, X_n be independent random variables such that $\mathbb{E}\{X_i\} = \bar{x}_i$ and $\text{Var}\{X_i\} \leq c < \infty$. Then, Tchebyshev's theorem states $\frac{1}{n} \sum_{n'=1}^n X_{n'} \xrightarrow[n \rightarrow \infty]{P} \frac{1}{n} \sum_{n'} \bar{x}_{n'}$.

³A sequence $\{X_n\}$ of random variables converges in probability to the random variable X if, for all $\epsilon > 0$, it holds that $\lim_{n \rightarrow \infty} \Pr(|X_n - X| > \epsilon) = 0$, where $\Pr(\cdot)$ denotes the probability of an event.

The assumptions in (24) and (25) imply that the largest singular value and the sum of the eigenvalues (counted with their multiplicity) of the $N \times N$ covariance matrices that characterize the spatial correlation among the channels of the RIS elements are finite and positive. Dividing both sides of (21) by MN and then applying Tchebyshev's theorem and (9), we obtain

$$\frac{1}{MN} \sum_{m=1}^M \sqrt{\eta_{k'}} \hat{u}_{mk}^* u_{mk'} \xrightarrow[M \rightarrow \infty]{N \rightarrow \infty} \frac{1}{MN} \sum_{m=1}^M \sqrt{\eta_{k'} p \tau_p} c_{mk} \text{tr}(\Phi^H \mathbf{R}_m \Phi \tilde{\mathbf{R}}_{mk'}). \quad (26)$$

We first observe that $\Phi^H \mathbf{R}_m \Phi \tilde{\mathbf{R}}_{mk'}$ is similar to $\tilde{\mathbf{R}}_{mk'}^{1/2} \Phi \mathbf{R}_m \Phi \tilde{\mathbf{R}}_{mk'}^{1/2}$, which is a positive semi-definite matrix.⁴ Because similar matrices have the same eigenvalues, it follows that $\text{tr}(\Phi^H \mathbf{R}_m \Phi \tilde{\mathbf{R}}_{mk'}) > 0$. Based on Assumption 1, we obtain the following inequalities

$$\frac{1}{N} \text{tr}(\Phi^H \mathbf{R}_m \Phi \tilde{\mathbf{R}}_{mk'}) \stackrel{(a)}{\leq} \frac{1}{N} \|\Phi\|_2 \text{tr}(\mathbf{R}_m \Phi \tilde{\mathbf{R}}_{mk'}) \stackrel{(b)}{=} \frac{1}{N} \text{tr}(\Phi \tilde{\mathbf{R}}_{mk'} \mathbf{R}_m) \stackrel{(c)}{\leq} \frac{1}{N} \|\tilde{\mathbf{R}}_{mk'}\|_2 \text{tr}(\mathbf{R}_m), \quad (27)$$

where (a) is obtained from Lemma 3 in Appendix A; (b) follows because $\|\Phi\|_2 = 1$; and (c) is obtained by applying again Lemma 3. Based on Assumption 1, the last inequality in (27) is bounded by a positive constant. From (26) and (27), therefore, the decision variable in (20) can be formulated as

$$\frac{1}{MN} r_{uk} \xrightarrow[M \rightarrow \infty]{N \rightarrow \infty} \frac{1}{MN} \sum_{k' \in \mathcal{P}_k} \sum_{m=1}^M \sqrt{\eta_{k'} p \tau_p} c_{mk} \text{tr}(\Phi^H \mathbf{R}_m \Phi \tilde{\mathbf{R}}_{mk'}) s_{k'}. \quad (28)$$

The expression obtained in (28) reveals that, as $M, N \rightarrow \infty$, the post-processed signal at the CPU consists of the desired signal of the intended user k and the interference from the other users in \mathcal{P}_k . Compared with (23), we observe that (28) is independent of the direct links and depends only on the RIS-assisted indirect links. This highlights the potentially promising contribution of the RIS, in the limiting regime $M, N \rightarrow \infty$, for enhancing the system performance.

C. Uplink Ergodic Net Throughput with a Finite Number of APs and RIS Elements

In this section, we focus our attention on the practical setup in which M and N are both finite. By utilizing the user-and-then forget channel capacity bounding method [35], the uplink ergodic net throughput of the user k can be written as follows

$$R_{uk} = B \nu_u (1 - \tau_u / \tau_p) \log_2 (1 + \text{SINR}_{uk}), [\text{Mbps}], \quad (29)$$

where B is the system bandwidth measured in MHz and $0 \leq \nu_u \leq 1$ is the portion of each coherence interval that is dedicated to the uplink data transmission. The effective uplink signal-to-noise-plus-interference ratio (SINR), which is denoted by SINR_{uk} , is defined as follows

$$\text{SINR}_{uk} = \frac{|\text{DS}_{uk}|^2}{\mathbb{E}\{|\text{BU}_{uk}|^2\} + \sum_{k'=1, k' \neq k}^K \mathbb{E}\{|\text{UI}_{uk'k}|^2\} + \mathbb{E}\{|\text{NO}_{uk}|^2\}}, \quad (30)$$

⁴Two matrices \mathbf{A} and \mathbf{B} of size $N \times N$ are similar if there exists an invertible $N \times N$ matrix \mathbf{U} such that $\mathbf{B} = \mathbf{U}^{-1} \mathbf{A} \mathbf{U}$.

where the following definitions hold

$$\begin{aligned} \text{DS}_{uk} &= \sqrt{\rho_u \eta_k} \mathbb{E} \left\{ \sum_{m=1}^M \hat{u}_{mk}^* u_{mk} \right\}, \text{BU}_{uk} = \sqrt{\rho_u \eta_k} \left(\sum_{m=1}^M \hat{u}_{mk}^* u_{mk} - \mathbb{E} \left\{ \sum_{m=1}^M \hat{u}_{mk}^* u_{mk} \right\} \right), \\ \text{UI}_{uk'k} &= \sqrt{\rho_u \eta_{k'}} \sum_{m=1}^M \hat{u}_{mk}^* u_{mk'}, \text{NO}_{uk} = \sum_{m=1}^M \hat{u}_{mk}^* w_{um}. \end{aligned} \quad (31)$$

In particular, DS_{uk} denotes the (average) strength of desired signal, BU_{uk} denotes the beamforming uncertainty, $\text{UI}_{uk'k}$ denotes the interference caused by the user k' to the user k , and NO_{uk} denotes the additive noise. We emphasize that the net throughput in (29) is achievable since it is a lower bound of the channel capacity. A closed-form expression for (29) is given in Theorem 1.

Theorem 1. *If the CPU utilizes the MR combining method, a lower-bound closed-form expression for the uplink net throughput of the user k is given by (29), where the SINR is*

$$\text{SINR}_{uk} = \frac{\rho_u \eta_k \left(\sum_{m=1}^M \gamma_{mk} \right)^2}{\text{CI}_{uk} + \text{NI}_{uk} + \text{NO}_{uk}}, \quad (32)$$

where CI_{uk} is the coherent interference, NI_{uk} is the non-coherent interference, and NO_{uk} is the noise, which are formulated as follows

$$\begin{aligned} \text{CI}_{uk} &= 2\rho_u p\tau_p \sum_{k' \in \mathcal{P}_k \setminus \{k\}} \sum_{m=1}^M \eta_{k'} c_{mk}^2 \xi_{mk'} + p\tau_p \rho_u \sum_{k' \in \mathcal{P}_k \setminus \{k\}} \eta_{k'} \left(\sum_{m=1}^M c_{mk} \delta_{mk'} \right)^2, \\ \text{NI}_{uk} &= 2\rho_u p\tau_p \sum_{m=1}^M \eta_k c_{mk}^2 \xi_{mk} + \rho_u \sum_{k'=1}^K \sum_{m=1}^M \eta_{k'} \gamma_{mk} \delta_{mk'}, \text{NO}_{uk} = \sum_{m=1}^M \gamma_{mk}, \end{aligned} \quad (33)$$

with $\xi_{mk'} = \text{tr}((\Phi^H \mathbf{R}_m \Phi \tilde{\mathbf{R}}_{mk'})^2)$, $\delta_{mk'} = \beta_{mk'} + \text{tr}(\Phi^H \mathbf{R}_m \Phi \tilde{\mathbf{R}}_{mk'})$, and γ_{mk} given in (13).

Proof. See Appendix D. □

By direct inspection of the SINR in (32), the numerator increases with the square of the sum of the variances of the channel estimates, γ_{mk} , $\forall m$ thanks to the joint coherent transmission, i.e., all the M APs transmit the same data to the user. On the other hand, the first term in the denominator represents the power of the coherent interference. Due to the limited and finite number of orthogonal pilot sequences being used, the second term in the denominator represents the impact of pilot contamination. The last term is the additive noise. If the coherence time is sufficiently large that every user can utilize its own orthogonal pilot sequence, the uplink net throughput of the user k can still be obtained from (29), but the effective SINR simplifies to

$$\text{SINR}_{uk} = \frac{\rho_u \eta_k \left(\sum_{m=1}^M \gamma_{mk}^o \right)^2}{2\rho_u p\tau_p \sum_{m=1}^M \eta_{k'} (c_{mk}^o)^2 \xi_{mk'} + \rho_u \sum_{k'=1}^K \sum_{m=1}^M \eta_{k'} \gamma_{mk}^o + \sum_{m=1}^M \gamma_{mk}^o}. \quad (34)$$

TABLE I

COMPARISON OF THE UPLINK SINR BETWEEN CELL-FREE MASSIVE MIMO AND RIS-ASSISTED CELL-FREE MASSIVE MIMO

Uplink SINR		Cell-Free Massive MIMO	RIS-Assisted Cell-Free Massive MIMO
(32)	c_{mk}	$\frac{\sqrt{p\tau_p}\beta_{mk}}{p\tau_p\sum_{k'\in\mathcal{P}_k}\beta_{mk'}+1}$	$\frac{\sqrt{p\tau_p}(\beta_{mk}+\text{tr}(\Phi^H\mathbf{R}_m\Phi\tilde{\mathbf{R}}_{mk}))}{p\tau_p\sum_{k'\in\mathcal{P}_k}(\beta_{mk'}+\text{tr}(\Phi^H\mathbf{R}_m\Phi\tilde{\mathbf{R}}_{mk'}))+1}$
	γ_{mk}	$\sqrt{p\tau_p}\beta_{mk}c_{mk}$	$\sqrt{p\tau_p}(\beta_{mk}+\text{tr}(\Phi^H\mathbf{R}_m\Phi\tilde{\mathbf{R}}_{mk}))c_{mk}$
	δ_{mk}	β_{mk}	$\beta_{mk}+\text{tr}(\Phi^H\mathbf{R}_m\Phi\tilde{\mathbf{R}}_{mk})$
	ξ_{mk}	-	$\text{tr}((\Phi^H\mathbf{R}_m\Phi\tilde{\mathbf{R}}_{mk})^2)$
	$ \text{DS}_{uk} ^2$	$\rho_u\eta_k\left(\sum_{m=1}^M\gamma_{mk}\right)^2$	$\rho_u\eta_k\left(\sum_{m=1}^M\gamma_{mk}\right)^2$
	CI_{uk}	$p\tau_p\rho_u\sum_{k'\in\mathcal{P}_k\setminus\{k\}}\eta_{k'}\left(\sum_{m=1}^M c_{mk}\delta_{mk'}\right)^2$	$2\rho_u p\tau_p\sum_{k'\in\mathcal{P}_k\setminus\{k\}}\sum_{m=1}^M\eta_{k'}c_{mk}^2\xi_{mk'}+p\tau_p\rho_u\sum_{k'\in\mathcal{P}_k\setminus\{k\}}\eta_{k'}\left(\sum_{m=1}^M c_{mk}\delta_{mk'}\right)^2$
	NI_{uk}	$\rho_u\sum_{k'=1}^K\sum_{m=1}^M\eta_{k'}\gamma_{mk}\delta_{mk'}$	$2\rho_u p\tau_p\sum_{m=1}^M\eta_k c_{mk}^2\xi_{mk}+\rho_u\sum_{k'=1}^K\sum_{m=1}^M\eta_{k'}\gamma_{mk}\delta_{mk'}$
	NO_{uk}	$\sum_{m=1}^M\gamma_{mk}$	$\sum_{m=1}^M\gamma_{mk}$
(34)	c_{mk}^o	$\frac{\sqrt{p\tau_p}\beta_{mk}}{p\tau_p\beta_{mk}+1}$	$\frac{\sqrt{p\tau_p}(\beta_{mk}+\text{tr}(\Phi^H\mathbf{R}_m\Phi\tilde{\mathbf{R}}_{mk}))}{p\tau_p(\beta_{mk}+\text{tr}(\Phi^H\mathbf{R}_m\Phi\tilde{\mathbf{R}}_{mk}))+1}$
	γ_{mk}^o	$\sqrt{p\tau_p}\beta_{mk}c_{mk}^o$	$\sqrt{p\tau_p}(\beta_{mk}+\text{tr}(\Phi^H\mathbf{R}_m\Phi\tilde{\mathbf{R}}_{mk}))c_{mk}^o$
	$ \text{DS}_{uk} ^2$	$\rho_u\eta_k\left(\sum_{m=1}^M\gamma_{mk}^o\right)^2$	$\rho_u\eta_k\left(\sum_{m=1}^M\gamma_{mk}^o\right)^2$
	CI_{uk}	-	-
	NI_{uk}	$\rho_u\sum_{k'=1}^K\sum_{m=1}^M\eta_{k'}\gamma_{mk}^o\delta_{mk'}$	$2\rho_u p\tau_p\sum_{m=1}^M\eta_k(c_{mk}^o)^2\xi_{mk}+\rho_u\sum_{k'=1}^K\sum_{m=1}^M\eta_{k'}\gamma_{mk}^o\delta_{mk'}$
	NO_{uk}	$\sum_{m=1}^M\gamma_{mk}^o$	$\sum_{m=1}^M\gamma_{mk}^o$

The SINR in (32) is a multivariate function of the matrix of phase shifts of the RIS and of the channel statistics, i.e., the channel covariance matrices. Table I gives a comparison of the uplink SINR expression of the user k with and without the presence of the RIS. By direct inspection of $|\text{DS}_{uk}|^2$, we evince that the strength of the desired signal gets better thanks to the assistance of the RIS. However, the coherent and non-coherent interference become more severe as well, due to the need of estimating both the direct and indirect links in the presence of the RIS. By assigning the orthogonal pilot sequences to all the K users, the coherent interference represented by CI_{uk} can be completely suppressed. In Section V, the performance of Cell-Free Massive MIMO and RIS-assisted Cell-Free Massive MIMO are compared with the aid of numerical simulations.

IV. DOWNLINK DATA TRANSMISSION AND PERFORMANCE ANALYSIS WITH MR PRECODING

In this section, we consider the downlink data transmission phase and analyze the received signal at the users when the number of APs is large. A closed-form expression of the downlink ergodic net throughput that is attainable with MR precoding and for an arbitrary phase shift matrix of the RIS elements is provided.

A. Downlink Data Transmission Phase

By exploiting channel reciprocity, the AP m treats the channel estimates obtained in the uplink as the true channels in order to construct the beamforming coefficients. Accordingly, the downlink

signal transmitted from the AP m is

$$x_m = \sqrt{\rho_d} \sum_{k=1}^K \sqrt{\eta_{mk}} \hat{u}_{mk}^* q_k, \quad (35)$$

where ρ_d is the normalized SNR in the downlink; q_k is the complex data symbol that is to be sent (cooperatively) by the M APs to the user k , with $\mathbb{E}\{|q_k|^2\} = 1$; and η_{mk} is the power control coefficient of the AP m , which satisfies the limited power budget constraint as follows

$$\mathbb{E}\{|x_m|^2\} \leq \rho_d \Rightarrow \sum_{k=1}^K \eta_{mk} \gamma_{mk} \leq 1. \quad (36)$$

The cooperation among the M APs for jointly transmitting the same data symbol to a particular user creates the major distinction between the downlink and uplink data transmission phases. Based on (35), the received signal at the user k is the superposition of the signals transmitted by the M APs as

$$r_{dk} = \sum_{m=1}^M u_{mk} x_m + w_{dk} = \sqrt{\rho_d} \sum_{m=1}^M \sum_{k'=1}^K \sqrt{\eta_{mk'}} u_{mk'} \hat{u}_{mk'}^* q_{k'} + w_{dk}. \quad (37)$$

where w_{dk} is the additive noise at the user k with $w_{dk} \sim \mathcal{CN}(0, 1)$. The user k decodes the desired data symbol based on the observation in (37).

B. Asymptotic Analysis of the Downlink Received Signal

In contrast with the uplink data processing where the CPU needs only the channel estimate \hat{u}_{mk} for detecting the data of the user k , as displayed in (20), the received signal in (37) depends on the channel estimates of the K users in the network, since the channel estimates from the K users are used for MR precoding. Therefore, the analysis of the uplink and downlink data transmission phases are different. First, we split (37) into three terms, by virtue of the pilot reuse pattern \mathcal{P}_k , as follows

$$r_{dk} = \sqrt{\rho_d} \sum_{k' \in \mathcal{P}_k} \sum_{m=1}^M \sqrt{\eta_{mk'}} u_{mk'} \hat{u}_{mk'}^* q_{k'} + \sqrt{\rho_d} \sum_{k' \notin \mathcal{P}_k} \sum_{m=1}^M \sqrt{\eta_{mk'}} u_{mk'} \hat{u}_{mk'}^* q_{k'} + w_{dk}. \quad (38)$$

Then, we investigate the two asymptotic regimes for $M \rightarrow \infty$ and $M, N \rightarrow \infty$ while keeping the M/N ratio fixed. In particular, the first term in (38) can be rewritten as

$$\begin{aligned} \sum_{m=1}^M \sqrt{\eta_{mk'}} u_{mk'} \hat{u}_{mk'}^* &\stackrel{(a)}{=} \sum_{m=1}^M \sqrt{\eta_{mk'}} c_{mk'} u_{mk} \left(\sum_{k'' \in \mathcal{P}_k} \sqrt{p_{\tau_p}} u_{mk''}^* + w_{pmk'}^* \right) \\ &\stackrel{(b)}{=} \sum_{m=1}^M \sqrt{\eta_{mk'}} p_{\tau_p} c_{mk'} |u_{mk}|^2 + \sum_{k'' \in \mathcal{P}_k \setminus \{k\}} \sum_{m=1}^M \sqrt{\eta_{mk'}} p_{\tau_p} c_{mk'} u_{mk} u_{mk''}^* + \sum_{m=1}^M \sqrt{\eta_{mk'}} c_{mk'} u_{mk} w_{pmk'}^*, \end{aligned} \quad (39)$$

where (a) is obtained by utilizing the channel estimates in (11) and (b) is obtained by extracting the aggregated channel of the user k from the summation. By letting M and/or N be large, similar to the uplink transmission phase, we obtain the following asymptotic results

$$\frac{1}{M} \sum_{m=1}^M \sqrt{\eta_{mk'}} u_{mk} \hat{u}_{mk'}^* \xrightarrow[M \rightarrow \infty]{P} \frac{1}{M} \sum_{m=1}^M \sqrt{\eta_{mk'}} p \tau_p c_{mk'} (\beta_{mk} + \text{tr}(\Phi^H \mathbf{R}_m \Phi \tilde{\mathbf{R}}_{mk})), \quad (40)$$

$$\frac{1}{MN} \sum_{m=1}^M \sqrt{\eta_{mk'}} u_{mk} \hat{u}_{mk'}^* \xrightarrow[N \rightarrow \infty]{M \rightarrow \infty, P} \frac{1}{MN} \sum_{m=1}^M \sqrt{\eta_{mk'}} p \tau_p c_{mk'} \text{tr}(\Phi^H \mathbf{R}_m \Phi \tilde{\mathbf{R}}_{mk}), \quad (41)$$

which are bounded based on Assumption 1. Consequently, the received signal at the user k converges to a deterministic equivalent as the number of APs is large, i.e., $M \rightarrow \infty$, and as the number of APs and RIS elements are large, i.e., $M, N \rightarrow \infty$, but their ratio is kept fixed. More precisely, the received signal converges (asymptotically) to

$$\frac{1}{M} r_{dk} \xrightarrow[M \rightarrow \infty]{P} \frac{1}{M} \sum_{k' \in \mathcal{P}_k} \sum_{m=1}^M \sqrt{\eta_{mk'}} p \tau_p c_{mk'} (\beta_{mk} + \text{tr}(\Phi^H \mathbf{R}_m \Phi \tilde{\mathbf{R}}_{mk})) s_{k'}, \quad (42)$$

$$\frac{1}{MN} r_{dk} \xrightarrow[M \rightarrow \infty]{P} \frac{1}{MN} \sum_{k' \in \mathcal{P}_k} \sum_{m=1}^M \sqrt{\eta_{mk'}} p \tau_p c_{mk'} \text{tr}(\Phi^H \mathbf{R}_m \Phi \tilde{\mathbf{R}}_{mk}) s_{k'}, \quad (43)$$

which indicates an inherent coexistence of the users in \mathcal{P}_k . The deterministic equivalents in (42) and (43) unveil that the impact of the channel estimation accuracy and the channel statistics is different between the uplink and the downlink. In particular, the asymptotic received signal in the uplink only depends on the channel estimation quality of each individual user, which is expressed by the coefficient c_{mk} . The asymptotic received signal in the downlink depends, on the other hand, on the channel estimation quality of all the users that share the same orthogonal pilot sequences, i.e., $c_{m,k'}, \forall k' \in \mathcal{P}_k$.

C. Downlink Ergodic Net Throughput with a Finite Number of APs and RIS Elements

By utilizing the channel capacity bounding technique [35], similar to the analysis of the uplink data transmission phase, the downlink ergodic net throughput of the user k can be written as follows

$$R_{dk} = B \nu_d (1 - \tau_p / \tau_c) \log_2 (1 + \text{SINR}_{dk}), [\text{Mbps}], \quad (44)$$

where $0 \leq \nu_d \leq 1$ is the portion of each coherence interval dedicated to the downlink data transmission, with $\nu_u + \nu_d = 1$, and the effective downlink SINR is defined as

$$\text{SINR}_{dk} = \frac{|\text{DS}_{dk}|^2}{\mathbb{E}\{|\text{BU}_{dk}|^2\} + \sum_{k'=1, k' \neq k}^K \mathbb{E}\{|\text{UI}_{dk'k}|^2\} + 1}, \quad (45)$$

where the following definitions hold

$$\begin{aligned} \text{DS}_{dk} &= \sqrt{\rho_d} \mathbb{E} \left\{ \sum_{m=1}^M \sqrt{\eta_{mk}} u_{mk} \hat{u}_{mk}^* \right\}, \quad \text{UI}_{dk'k} = \sqrt{\rho_d} \sum_{m=1}^M \sqrt{\eta_{mk'}} u_{mk} \hat{u}_{mk'}^*, \\ \text{BU}_{dk} &= \sqrt{\rho_d} \left(\sum_{m=1}^M \sqrt{\eta_{mk}} u_{mk} \hat{u}_{mk}^* - \mathbb{E} \left\{ \sum_{m=1}^M \sqrt{\eta_{mk}} u_{mk} \hat{u}_{mk}^* \right\} \right), \end{aligned} \quad (46)$$

In particular, DS_{dk} denotes the (average) strength of the desired signal received by the user k , BU_{dk} denotes the beamforming uncertainty, $\text{UI}_{dk'k}$ denotes the interference caused to the user k by the signal intended to the user k' . The downlink ergodic net throughput in (44) is achievable since it is a lower bound of the channel capacity, similar to the uplink data transmission. In contrast to the uplink ergodic net throughput, which only depends on the combining coefficients of each individual user, the downlink net throughput of the user k depends on the precoding coefficients of all the K users. A closed-form expression for (44) is given in Theorem 2.

Theorem 2. *If the CPU utilizes the MR precoding method, a lower-bound closed-form expression for the downlink net throughput of the user k is given by (44), where the SINR is*

$$\text{SINR}_{dk} = \frac{\rho_d \left(\sum_{m=1}^M \sqrt{\eta_{mk}} \gamma_{mk} \right)^2}{\text{CI}_{dk} + \text{NI}_{dk} + 1}, \quad (47)$$

where CI_{dk} is the coherent interference and NI_{dk} is the non-coherent interference, which are defined as follows

$$\text{CI}_{dk} = 2\rho_d p \tau_p \sum_{k' \in \mathcal{P}_k \setminus \{k\}} \sum_{m=1}^M \eta_{mk'} c_{mk'}^2 \xi_{mk} + \rho_d p \tau_p \sum_{k' \in \mathcal{P}_k \setminus \{k\}} \left(\sum_{m=1}^M \sqrt{\eta_{mk'}} c_{mk'} \delta_{mk} \right)^2, \quad (48)$$

$$\text{NI}_{dk} = 2\rho_d p \tau_p \sum_{m=1}^M \eta_{mk} c_{mk}^2 \xi_{mk} + \rho_d \sum_{k'=1}^K \sum_{m=1}^M \eta_{mk'} \gamma_{mk'} \delta_{mk}. \quad (49)$$

Proof. The main steps of the proof are similar to those of the proof of Theorem 1. However, there are also major differences that are due to the coherent joint data transmission among the APs. The details of the proof are available in Appendix E. \square

From Theorem 2, we observe that the effective downlink SINR has some similarities and differences as compared with its uplink counterpart in Theorem 1. Similar to the uplink, the numerator of (47) is a quadratic function that depends on the channel estimation quality and the coherent joint transmission processing. Differently from the uplink, the transmit power coefficients appear explicitly in the numerator of (47) as a result of the cooperation among the APs. The first term in the denominator of (47) unveils the impact of pilot contamination. In contrast to the uplink, we observe that it depends on all the transmit power coefficients. In addition, we observe that the impact of pilot contamination

TABLE II
COMPARISON OF THE DOWNLINK SINR BETWEEN CELL-FREE MASSIVE MIMO AND RIS-ASSISTED CELL-FREE MASSIVE MIMO (SOME PARAMETERS ARE DEFINED IN TABLE I)

Downlink SINR		Cell-Free Massive MIMO	RIS-Assisted Cell-Free Massive MIMO
(47)	$ \text{DS}_{dk} ^2$	$\rho_d \left(\sum_{m=1}^M \sqrt{\eta_{mk}} \gamma_{mk} \right)^2$	$\rho_d \left(\sum_{m=1}^M \sqrt{\eta_{mk}} \gamma_{mk} \right)^2$
	CI_{dk}	$\rho_d p \tau_p \sum_{k' \in \mathcal{P}_k \setminus \{k\}} \left(\sum_{m=1}^M \sqrt{\eta_{mk'}} c_{mk'} \delta_{mk} \right)^2$	$2\rho_d p \tau_p \sum_{k' \in \mathcal{P}_k \setminus \{k\}} \sum_{m=1}^M \eta_{mk'} c_{mk'}^2 \xi_{mk} + \rho_d p \tau_p \sum_{k' \in \mathcal{P}_k \setminus \{k\}} \left(\sum_{m=1}^M \sqrt{\eta_{mk'}} c_{mk'} \delta_{mk} \right)^2$
	NI_{dk}	$\rho_d \sum_{k'=1}^K \sum_{m=1}^M \eta_{mk'} \gamma_{mk'} \delta_{mk}$	$2\rho_d p \tau_p \sum_{m=1}^M \eta_{mk} c_{mk}^2 \xi_{mk} + \rho_d \sum_{k'=1}^K \sum_{m=1}^M \eta_{mk'} \gamma_{mk'} \delta_{mk}$
	NO_{dk}	1	1
(50)	$ \text{DS}_{dk} ^2$	$\rho_d \left(\sum_{m=1}^M \sqrt{\eta_{mk}} \gamma_{mk}^o \right)^2$	$\rho_d \left(\sum_{m=1}^M \sqrt{\eta_{mk}} \gamma_{mk}^o \right)^2$
	CI_{dk}	-	-
	NI_{dk}	$\rho_d \sum_{k'=1}^K \sum_{m=1}^M \eta_{mk'} \gamma_{mk'}^o \delta_{mk}$	$2\rho_d p \tau_p \sum_{m=1}^M \eta_{mk} (c_{mk}^o)^2 \xi_{mk} + \rho_d \sum_{k'=1}^K \sum_{m=1}^M \eta_{mk'} \gamma_{mk'}^o \delta_{mk}$
	NO_{dk}	1	1

scales up with the number of APs and with the number of elements of the RIS. Finally, the second term accounts for the non-coherent interference from the other users in the network. When the K users employ orthogonal pilot sequences, the downlink SINR expression of the user k simplifies to

$$\text{SINR}_{dk} = \frac{\rho_d \left(\sum_{m=1}^M \sqrt{\eta_{mk}} \gamma_{mk} \right)^2}{2\rho_d p \tau_p \sum_{m=1}^M \eta_{mk} (c_{mk}^o)^2 \xi_{mk} + \rho_d \sum_{k'=1}^K \sum_{m=1}^M \eta_{mk'} \gamma_{mk'}^o \delta_{mk} + 1}. \quad (50)$$

A comparison of the downlink SINR for Cell-Free Massive MIMO and RIS-assisted Cell-Free Massive MIMO systems is given in Table II. By comparing Table I and Table II, the difference and similarities between the uplink and downlink transmission phases can be identified as well. With the aid of numerical results, in Section V, we will illustrate the advantages of RIS-assisted Cell-Free Massive MIMO especially if the direct links are not sufficiently reliable (e.g., they are blocked) with high probability.

Remark 2. We observe that the ergodic net throughput in the uplink (Theorem 1) and downlink (Theorem 2) data transmission phases depend only on the large-scale fading statistics and on the channel covariance matrices, while they are independent of the instantaneous CSI. This simplifies the deployment and optimization of RIS-assisted Cell Free Massive MIMO systems. As anticipated in Remark 1, in fact, the phase shifts of the RIS can be optimized based on the (long-term) analytical expressions of the ergodic net throughputs in Theorem 1 and Theorem 2, which are independent of the instantaneous CSI. In this paper, we have opted for optimizing the phase shifts of the RIS in order to minimize the channel estimation error, which determines the performance of both the uplink and downlink transmission phases. The optimization of the phase shifts of the RISs based on the closed-form expressions in Theorem 1 and Theorem 2 is postponed to a future research work.

V. NUMERICAL RESULTS

In this section, we report some numerical results in order to illustrate the performance of the RIS-assisted Cell-Free Massive MIMO system introduced in the previous sections. We consider a geographic area of size 1 km^2 , where the locations of the APs and users are given in terms of (x, y) coordinates. The four vertices of the considered region are $[-0.5, -0.5] \text{ km}$, $[-0.5, 0.5] \text{ km}$, $[0.5, 0.5] \text{ km}$, $[0.5, -0.5] \text{ km}$. To minimize the border effects, the considered region is wrapped around at the edges. To simulate a harsh communication environment, the M APs are uniformly distributed in the sub-region $x, y \in [-0.5, -0.25] \text{ km}$, while the K users are uniformly distributed in the sub-region $x, y \in [0.25, 0.25] \text{ km}$. The RIS is located at the origin, i.e., $(x, y) = (0, 0)$. The carrier frequency is 1.9 GHz and the system bandwidth is 20 MHz. Each coherence interval comprises $\tau_c = 200$ symbols, which may correspond to a coherence bandwidth $B_c = 200 \text{ KHz}$ and a coherence time $T_c = 1 \text{ ms}$. We assume $\tau_p = 5$ orthonormal pilot sequences that are shared by all the users. The large-scale fading coefficients in dB are generated according to the three-slope propagation model in [7], where the path loss exponent depends on the distance between the transmitter and the receiver. The shadow fading has a log-normal distribution with standard deviation equal to 8 dB. The distance thresholds for the three slopes are 10 m and 50 m. The height of the APs, RIS, and users is 15 m, 30 m, and 1.65 m, respectively. The direct links, $g_{mk}, \forall m, k$, are assumed to be unblocked with a given probability. More specifically, the large-scale fading coefficient β_{mk} is formulated as follows

$$\beta_{mk} = \bar{\beta}_{mk} a_{mk}, \quad (51)$$

where $\bar{\beta}_{mk}$ accounts for the path loss due to the transmission distance and the shadow fading according to the three-slope propagation model in [7]. The binary variables a_{mk} accounts for the probability that the direct links are unblocked, and it is defined as

$$a_{mk} = \begin{cases} 1, & \text{with a probability } p, \\ 0, & \text{with a probability } 1 - p, \end{cases} \quad (52)$$

where $p \in [0, 1]$ is the probability that the direct link is not blocked. The noise variance is -92 dBm , which corresponds to a noise figure of 9 dB. The covariance matrices are generated according to the spatial correlation model in (2). The power of the pilot sequences is 100 mW and the power budget of each AP is 200 mW. The time intervals of data transmission, in each coherence interval, that is allocated for the uplink and downlink transmissions are $\nu_u = \nu_d = 0.5$. The uplink and downlink power control coefficients are $\eta_k = 1, \forall k$, and $\eta_{mk} = (\sum_{k'=1}^K \gamma_{mk'})^{-1}, \forall m, k$.⁵ As far as the optimization of the phase shifts of the RIS elements are concerned, we assume that they are optimized according

⁵In the worst case, if all the direct links are blocked, we introduce a damping constant when Cell-Free Massive MIMO systems in the absence of RIS are considered, since in those cases we have $\sum_{m=1}^M \gamma_{mk'} = 0$.

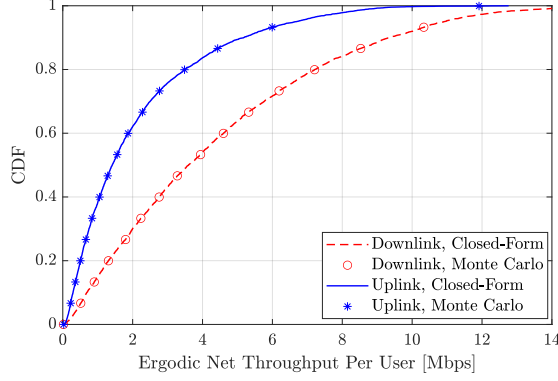


Fig. 2. Monte Carlo simulations versus the analytical frameworks with $M = 20$, $K = 5$, $N = 64$, $\tau_p = 2$, and $d_H = d_V = \lambda/4$. The unblocked probability of the direct links is $p = 1.0$.

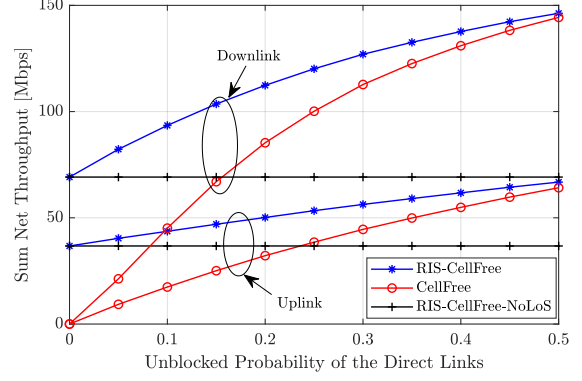


Fig. 3. The sum net throughput [Mbps] versus the unblocked probability of the direct links p with $M = 100$, $K = 10$, $N = 900$, $\tau_p = 5$, and $d_H = d_V = \lambda/4$.

to the sum-NMSE minimization criterion in the absence of direct links, according to Corollary 1 and Remark 1. Without loss of generality, in particular, the N phase shifts in Φ are all set equal to $\pi/4$, except in Figs. 5 and 6 where different phase shifts are considered for comparison. In order to evaluate the advantages and limitations of RIS-assisted Cell-Free Massive MIMO systems, three system configurations are considered for comparison:

- i) *RIS-Assisted Cell-Free Massive MIMO*: This is the proposed system model in which the direct links are blocked according to (52). This setup is denoted by “RIS-CellFree”.
- ii) *(Conventional) Cell-Free Massive MIMO*: This setup is the same as the previous one with the only exception that the RIS is not deployed in the network. This setup is denoted by “CellFree”.
- iii) *RIS-Assisted Cell-Free Massive MIMO with blocked direct links*: This is the worst case study in which the direct links are blocked with unit probability and the uplink and downlink transmissions are ensured only through the RIS. This setup is denoted by “RIS-CellFree-NoLoS”.

In Fig. 2, we illustrate the cumulative distribution function (CDF) obtained by using Monte Carlo methods from (29) and (44), and the analytical expressions of the net throughput obtained in Theorem 1 and Theorem 2. We observe a very good overlap between the numerical simulations and the obtained analytical expressions. From Fig. 2, we evince that the downlink net throughput per user is about $2.1\times$ better than the uplink net throughput. This is due to the higher transmission power of the APs and the gain of the joint processing gain of the APs. Since the Monte Carlo simulations are not simple to obtain for larger values of the simulation parameters, the rest of the figures are obtained only by using the closed-form expressions derived in Theorem 1 and Theorem 2.

In Fig. 3 we illustrate the sum net throughput as a function of the probability p in (52). In particular, the uplink sum net throughput is defined as $\sum_{k=1}^K R_{uk}$ and the downlink sum net throughput is defined as $\sum_{k=1}^K R_{dk}$. From the obtained results, we evince that Cell-Free Massive MIMO provides the worst performance if the blocking probability is large (p is small). If the direct links are unreliable, as

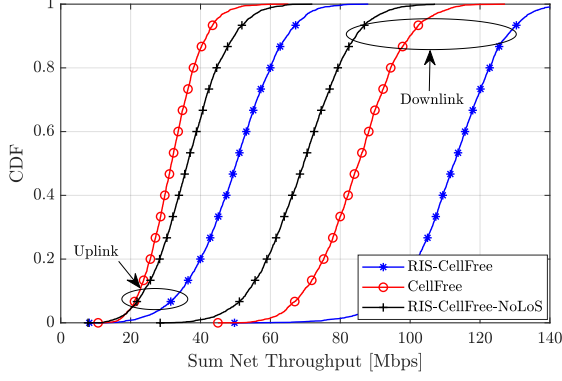


Fig. 4. CDF of the sum net throughput [Mbps] with $M = 100$, $K = 10$, $N = 900$, $\tau_p = 5$, and $d_H = d_V = \lambda/4$. The unblocked probability of the direct links is $p = 0.2$.

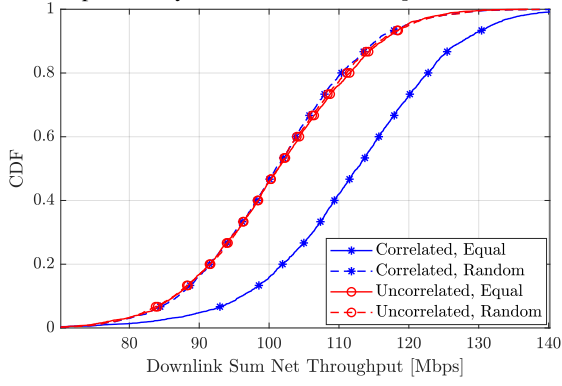


Fig. 6. CDF of the downlink sum net throughput [Mbps] with $M = 100$, $K = 10$, $N = 900$, $\tau_p = 5$, and $d_H = d_V = \lambda/4$. The unblocked probability of the direct links is $p = 0.2$.

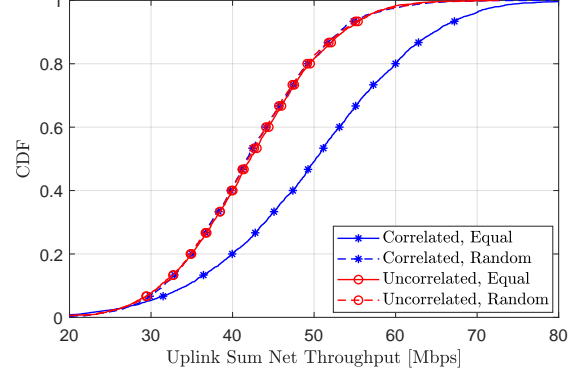


Fig. 5. CDF of the uplink sum net throughput [Mbps] with $M = 100$, $K = 10$, $N = 900$, $\tau_p = 5$, and $d_H = d_V = \lambda/4$. The unblocked probability of the direct links is $p = 0.2$.

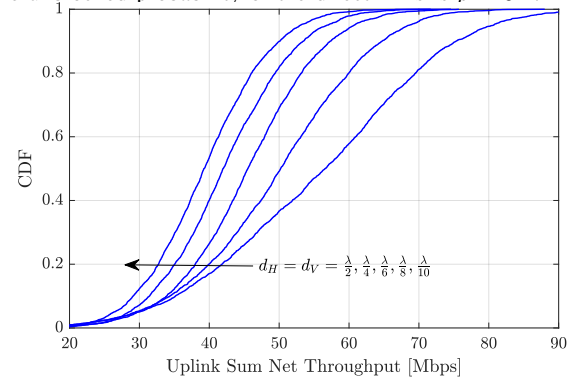


Fig. 7. CDF of the uplink sum net throughput [Mbps] with the different $\{d_H, d_V\}$, $M = 100$, $K = 10$, $N = 900$, and $\tau_p = 5$. The unblocked probability of the direct links is $p = 0.2$.

expected, the net throughput offered by Cell-Free Massive MIMO tends to zero if $p \rightarrow 0$. By assuming $p = 0.1$, for example, Cell Free Massive MIMO is approximately $2.1\times$ and $1.6\times$ worse than the worst-case RIS-assisted Cell-Free Massive MIMO setup (RIS-CellFree-NoLoS) in the uplink and downlink, respectively. In the considered case study, in addition, we note that the proposed RIS-assisted Cell-Free Massive MIMO setup offers the best net throughput, since it can overcome the unreliability of the direct links thanks to the presence of the RIS. The presence of the RIS is particularly useful if p is small, i.e., $p < 0.2$ in Fig. 3, since in this case the direct links are not able to support a high throughput. In this case, the combination of Cell-Free Massive MIMO and RISs is capable of providing a high throughput and signal reliability.

In Fig. 4, we compare the three considered systems in terms of sum net throughput when $p = 0.2$. We observe the net advantage of the proposed RIS-assisted Cell-Free Massive MIMO system, especially in the downlink. In the uplink, in addition, even the worst-case RIS-assisted Cell-Free Massive MIMO system setup (i.e., $p = 0$) outperforms the Cell-Free Massive MIMO setup in the absence of an RIS. In the following figures, we focus our attention only on the RIS-assisted Cell-Free

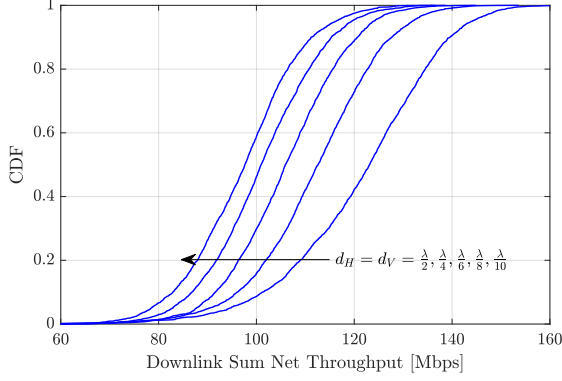


Fig. 8. The CDF of downlink sum net throughput [Mbps] with the different $\{d_H, d_V\}$, $M = 100$, $K = 10$, $N = 900$, and $\tau_p = 5$. The unblocked probability of the direct links is $p = 0.2$.

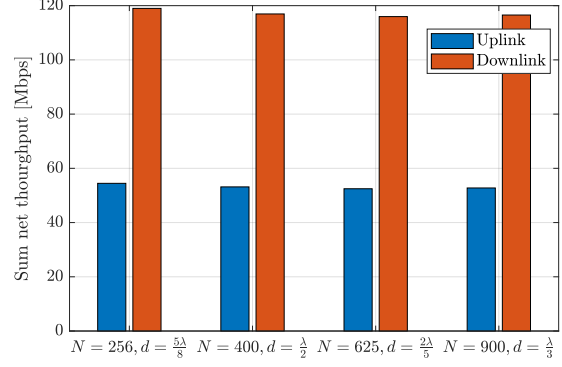


Fig. 9. The CDF of sum net throughput [Mbps] with $M = 100$, $K = 10$, and $\tau_p = 5$. Here, $d = d_H = d_V$ and the unblocked probability of the direct links is $p = 0.2$.

Massive MIMO setup, since it provides the best performance.

In Figs. 5 and 6, we compare the uplink and downlink sum net throughput as a function of the phase shifts of the RISs (random and uniform phase shifts according to Corollary 1) in the presence of spatially-correlated and spatially-independent fading channels according to (2). In the presence of spatial correlation, we consider $\mathbf{R}_m = \alpha_m d_H d_V \mathbf{I}_N$ and $\tilde{\mathbf{R}}_{mk} = \tilde{\alpha}_{mk} d_H d_V \mathbf{I}_N, \forall m, k$. We note different performance trends in spatially-correlated fading channels. If the spatial correlation is not considered, we observe that there is no significant difference between the random and uniform phase shifts setup. In the presence of spatial correlation, on the other hand, the proposed uniform phase shift design that is obtained from Corollary 1 provides a much better throughput. This result highlights the relevance of using even simple optimization designs for RIS-assisted communications in the presence of spatial correlation.

In Figs. 7 and 8, we analyze the impact of the size of the scattering elements of the RISs on the uplink and downlink net throughputs, respectively, while keeping the number N of RIS elements fixed. The size of the considered RIS, which is a compact surface, is $N d_H d_V$, which implies that it increases as the size $d_H d_V$ of each element of the RIS increases. In this setup, we observe that the net throughput increases as the physical size of each radiating element of the RIS increases. In Fig. 9, on the other hand, we analyze a setup in which the total size of the RIS is kept constant to $N d_H d_V = 10\lambda \times 10\lambda$ and the triplet $(N, d = d_H = d_V)$ is changed accordingly. With the considered fading spatial correlation model and for a size of the RIS elements no smaller than $\lambda/3$, we do not observe a significant difference of the achievable net throughput. Further studies are, however, necessary for deep sub-wavelength RIS structures, for different optimization criteria of the phase shifts of the RISs, and in the presence of mutual coupling in addition to the fading spatial correlation [36], [37].

VI. CONCLUSION

Cell-Free Massive MIMO and RIS are two disruptive technologies for boosting the system performance of future wireless networks. These two technologies are not competing with each other, but have complementary features that can be integrated and leveraged to enhance the system performance in harsh communication environments. Therefore, we have considered an RIS-assisted Cell-Free Massive MIMO system that operates according to the TDD mode. An efficient channel estimation scheme has been introduced to overcome the high overhead that may be associated with the estimation of the individual channels of the RIS elements. Based on the proposed channel estimation scheme, an optimal design for the phase shifts of the RIS that minimizes the channel estimation error has been devised and has been used for system analysis. Based on the proposed channel estimation method, closed-form expressions of the ergodic net throughput for the uplink and downlink data transmission phases have been proposed. Based on them, the performance of RIS-assisted Cell-Free Massive MIMO has been analyzed as a function of the fading spatial correlation and the blocking probability of the direct AP-user links. The numerical results have shown that the presence of an RIS is particularly useful if the AP-user links are unreliable with high probability.

Possible generalizations of the results illustrated in this paper include the optimization of the phase shifts of the RIS that maximize the uplink or downlink throughput, the analysis of the impact of the fading spatial correlation for non-compact and deep sub-wavelength RIS structures, and the analysis and optimization of RIS-assisted systems in the presence of mutual coupling.

APPENDIX

A. Useful Lemmas

This appendix reports the two useful lemmas that are utilized for asymptotic analyses and as well as the proof of the theorems and lemmas given throughout the paper.

Lemma 3. [38, Lemma B.7] *For an arbitrary matrix $\mathbf{X} \in \mathbb{C}^{N \times N}$ and a positive semi-definite matrix $\mathbf{Y} \in \mathbb{C}^{N \times N}$, it holds that $|\text{tr}(\mathbf{X}\mathbf{Y})| \leq \|\mathbf{X}\|_2 \text{tr}(\mathbf{Y})$. If \mathbf{X} is also a positive semi-definite matrix, then $\text{tr}(\mathbf{X}\mathbf{Y}) \leq \|\mathbf{X}\|_2 \text{tr}(\mathbf{Y})$.*

Lemma 4. [39, Lemma 9] *For a random variable $\mathbf{x} \in \mathbb{C}^N$ distributed as $\mathcal{CN}(\mathbf{0}, \mathbf{R})$ with $\mathbf{R} \in \mathbb{C}^{N \times N}$ and a given deterministic matrix $\mathbf{M} \in \mathbb{C}^{N \times N}$, it holds that $\mathbb{E}\{|\mathbf{x}^H \mathbf{M} \mathbf{x}|^2\} = |\text{tr}(\mathbf{R}\mathbf{M})|^2 + \text{tr}(\mathbf{R}\mathbf{M}\mathbf{R}\mathbf{M}^H)$.*

B. Proof of Lemma 1

We first compute the second moment of the aggregated channel u_{mk} by capitalizing on the statistical independence of the direct and indirect channels, as follows

$$\begin{aligned} \mathbb{E}\{|u_{mk}|^2\} &= \mathbb{E}\{|g_{mk}|^2\} + \mathbb{E}\{|\mathbf{h}_m^H \Phi \mathbf{z}_{mk}|^2\} \stackrel{(a)}{=} \beta_{mk} + \mathbb{E}\{\text{tr}(\Phi^H \mathbf{h}_m \mathbf{h}_m^H \Phi \mathbf{z}_{mk} \mathbf{z}_{mk}^H)\} \\ &\stackrel{(b)}{=} \beta_{mk} + \text{tr}(\Phi^H \mathbb{E}\{\mathbf{h}_m \mathbf{h}_m^H\} \Phi \mathbb{E}\{\mathbf{z}_{mk} \mathbf{z}_{mk}^H\}) = \beta_{mk} + \text{tr}(\Phi^H \mathbf{R}_m \Phi \tilde{\mathbf{R}}_{mk}), \end{aligned} \quad (53)$$

where (a) follows by applying the trace of product property $\text{tr}(\mathbf{X}\mathbf{Y}) = \text{tr}(\mathbf{Y}\mathbf{X})$ for some given size-matched matrices \mathbf{X} and \mathbf{Y} ; and (b) is obtained thanks to the independence of the cascaded channels \mathbf{h}_m and \mathbf{z}_{mk} . The fourth moment of the aggregated channel can be written, from (8), as follows

$$\mathbb{E}\{|u_{mk}|^4\} = \mathbb{E}\left\{\left|g_{mk}|^2 + g_{mk}^* \mathbf{h}_m^H \Phi \mathbf{z}_{mk} + g_{mk} \mathbf{z}_{mk}^H \Phi^H \mathbf{h}_m + |\mathbf{h}_m^H \Phi \mathbf{z}_{mk}|^2\right|^2\right\} \quad (54)$$

By setting $a = |g_{mk}|^2$, $b = g_{mk}^* \mathbf{h}_m^H \Phi \mathbf{z}_{mk}$, $c = g_{mk} \mathbf{z}_{mk}^H \Phi^H \mathbf{h}_m$, and $d = |\mathbf{h}_m^H \Phi \mathbf{z}_{mk}|^2$, (54) can be equivalently written as follows

$$\mathbb{E}\{|u_{mk}|^4\} = \mathbb{E}\{|a|^4\} + \mathbb{E}\{|b|^2\} + \mathbb{E}\{|c|^2\} + 2\mathbb{E}\{ad\} + \mathbb{E}\{|d|^4\}. \quad (55)$$

By applying Lemma 4 with $g_{mk} \sim \mathcal{CN}(0, \beta_{mk})$, the first expectation in the right-hand side of (55) is equal to

$$\mathbb{E}\{|a|^4\} = 2\beta_{mk}^2. \quad (56)$$

By exploiting the independence between the direct and RIS-assisted links, the next three expectations in the right-hand side of (55) are equal to

$$\mathbb{E}\{|b|^2\} = \mathbb{E}\{|c|^2\} = \mathbb{E}\{ad\} = \beta_{mk} \text{tr}(\Phi^H \mathbf{R}_m \Phi \tilde{\mathbf{R}}_{mk}). \quad (57)$$

By introducing the normalized variable $\tilde{z} = \mathbf{h}_m^H \Phi \mathbf{z}_{mk} / \|\mathbf{R}_m^{1/2} \Phi \mathbf{z}_{mk}\|$ with $\tilde{z} \sim \mathcal{CN}(0, 1)$, the last expectation in the right-hand side of (55) is equal to

$$\begin{aligned} \mathbb{E}\{|d|^2\} &= \mathbb{E}\left\{\|\mathbf{R}_m^{1/2} \Phi \mathbf{z}_{mk}\|^4 |\tilde{z}|^4\right\} \stackrel{(a)}{=} \mathbb{E}\left\{\|\mathbf{R}_m^{1/2} \Phi \mathbf{z}_{mk}\|^4\right\} \mathbb{E}\{|\tilde{z}|^4\} \\ &= 2 \left(\text{tr}(\Phi^H \mathbf{R}_m \Phi \tilde{\mathbf{R}}_{mk})\right)^2 + 2\text{tr}\left((\Phi^H \mathbf{R}_m \Phi \tilde{\mathbf{R}}_{mk})^2\right), \end{aligned} \quad (58)$$

where (a) follows because \tilde{z} is independent of the remaining random variables; and (b) is obtained by virtue of Lemma 4. Plugging (56)–(58) into (55), the proof follows with the aid of some algebraic manipulations.

C. Proof of Corollary 1

We introduce the shorthand notation $b_{mk} = p\tau_p \alpha_m \tilde{\alpha}_{mk} d_H^2 d_V^2$ and $d_{mk} = p\tau_p d_H^2 d_V^2 \alpha_m \sum_{k' \in \mathcal{P}_k} \tilde{\alpha}_{mk'}$. When the direct links are weak enough to be negligible, the NMSE of the channel estimate of the user k at the AP m can be reformulated as follows

$$\text{NMSE}_{mk} = 1 - \frac{b_{mk} \text{tr}(\Phi^H \mathbf{R} \Phi \mathbf{R})}{1 + d_{mk} \text{tr}(\Phi^H \mathbf{R} \Phi \mathbf{R})}. \quad (59)$$

Let us denote by $f(\text{tr}(\Phi^H \mathbf{R} \Phi \mathbf{R})) = \sum_{m=1}^M \sum_{k=1}^K \text{NMSE}_{mk}$ the objective function of the problem in (17), the first-order derivative of NMSE_{mk} with respect to $\text{tr}(\Phi^H \mathbf{R} \Phi \mathbf{R})$ is

$$\frac{df(\text{tr}(\Phi^H \mathbf{R} \Phi \mathbf{R}))}{d\text{tr}(\Phi^H \mathbf{R} \Phi \mathbf{R})} = - \sum_{m=1}^M \sum_{k=1}^K \frac{b_{mk}}{(1 + d_{mk} \text{tr}(\Phi^H \mathbf{R} \Phi \mathbf{R}))^2} < 0, \quad (60)$$

which implies the objective function is a monotonically decreasing function of $\text{tr}(\Phi^H \mathbf{R} \Phi \mathbf{R})$ since $b_{mk} \geq 0, \forall m, k$. Moreover, $\Phi^H \mathbf{R} \Phi \mathbf{R}$ is similar to $\mathbf{R}^{1/2} \Phi^H \mathbf{R} \Phi \mathbf{R}^{1/2}$, which is a positive semidefinite matrix. Thus, we obtain

$$\text{tr}(\Phi^H \mathbf{R} \Phi \mathbf{R}) = |\text{tr}(\Phi^H \mathbf{R} \Phi \mathbf{R})| = \left| \sum_{n=1}^N \sum_{n'=1}^N (r^{nn'})^2 e^{j(\theta_n - \theta_{n'})} \right| \stackrel{(a)}{\leq} \sum_{n=1}^N \sum_{n'=1}^N (r^{nn'})^2, \quad (61)$$

where (a) is obtained by utilizing Cauchy-Schwarz's inequality, which holds with equality if $\theta_n = \theta_{n'}, \forall n, n'$. By combining (60) and (61), the proof is concluded.

D. Proof of Theorem 1

To obtain the closed-form expression of the uplink SINR in (30), we first compute $|\text{DS}_k|^2$ by using the definition of u_{mk} in (8) as

$$|\text{DS}_k|^2 \stackrel{(a)}{=} \rho_u \eta_k \left| \mathbb{E} \left\{ \sum_{m=1}^M \hat{u}_{mk}^* (\hat{u}_{mk} + e_{mk}) \right\} \right|^2 \stackrel{(b)}{=} \rho_u \eta_k \left| \sum_{m=1}^M \mathbb{E} \{ |\hat{u}_{mk}|^2 \} \right|^2 = \rho_u \eta_k \left(\sum_{m=1}^M \gamma_{mk} \right)^2, \quad (62)$$

where (a) is obtained by expressing the original channel u_{mk} into the summation of its channel estimate and its estimation error as stated in Lemma 2; and (b) is obtained by the fact that the channel estimate and the estimation error are uncorrelated. Since the variance of the summation of independent random variables is equal to the sum of the variances, the first expectation in the denominator of (30) is equal to

$$\begin{aligned} \mathbb{E}\{|\text{BU}_k|^2\} &= \rho_u \eta_k \sum_{m=1}^M \mathbb{E} \{ |\hat{u}_{mk}^* u_{mk} - \mathbb{E} \{ \hat{u}_{mk}^* u_{mk} \}|^2 \} \stackrel{(a)}{=} \rho_u \eta_k \sum_{m=1}^M \mathbb{E} \{ |\hat{u}_{mk}^* u_{mk}|^2 \} \\ &\quad - \rho_u \eta_k \sum_{m=1}^M |\mathbb{E} \{ \hat{u}_{mk}^* u_{mk} \}|^2 = \rho_u \eta_k \sum_{m=1}^M \mathbb{E} \{ |\hat{u}_{mk}^* u_{mk}|^2 \} - \rho_u \eta_k \sum_{m=1}^M \gamma_{mk}^2, \end{aligned} \quad (63)$$

where (a) is obtained by using the identity $\mathbb{E}\{|X - \mathbb{E}\{X\}|^2\} = \mathbb{E}\{|X|^2\} - |\mathbb{E}\{X\}|^2$; and (b) is obtained from $u_{mk}^* = \hat{u}_{mk}^* + e_{mk}^*$ by taking into account that the channel estimate and estimation error are uncorrelated random variables as stated in Lemma 2. By replacing $\hat{u}_{mk}^* = c_{mk} y_{pmk}^*$ in the first expectation of (63), we obtain

$$\begin{aligned} \mathbb{E} \{ |\hat{u}_{mk}^* u_{mk}|^2 \} &= c_{mk}^2 \mathbb{E} \{ |y_{pmk}^* u_{mk}|^2 \} = c_{mk}^2 \mathbb{E} \left\{ \left| \left(\sum_{k' \in \mathcal{P}_k} \sqrt{p\tau_p} u_{mk'}^* + w_{pmk}^* \right) u_{mk} \right|^2 \right\} \\ &= \underbrace{c_{mk}^2 p\tau_p \mathbb{E}\{|u_{mk}|^4\}}_{=T_{11}} + \underbrace{c_{mk}^2 p\tau_p \sum_{k' \in \mathcal{P}_k \setminus \{k\}} \mathbb{E}\{|u_{mk'}^* u_{mk}|^2\}}_{=T_{12}} + \underbrace{c_{mk}^2 \mathbb{E}\{|w_{pmk}^* u_{mk}|^2\}}_{=T_{13}}. \end{aligned} \quad (64)$$

Let us now analyze the three terms in the last equality of (64). The first term can be computed by exploiting the fourth moment given in (10), as follows

$$T_{11} = 2c_{mk}^2 p\tau_p \delta_{mk}^2 + 2c_{mk}^2 p\tau_p \xi_{mk} \stackrel{(a)}{=} \gamma_{mk}^2 + c_{mk}^2 p\tau_p \delta_{mk}^2 + 2c_{mk}^2 p\tau_p \xi_{mk}, \quad (65)$$

where (a) is obtained by using the variance of the channel estimate in (13), with δ_{mk} and ξ_{mk} defined in the statement of the theorem. The second term can be computed by exploiting the uncorrelation of the two cascaded channels, as follows

$$T_{12} = c_{mk}^2 p \tau_p \sum_{k' \in \mathcal{P}_k \setminus \{k\}} \mathbb{E}\{|u_{mk'}|^2\} \mathbb{E}\{|u_{mk}|^2\} = c_{mk}^2 p \tau_p \sum_{k' \in \mathcal{P}_k \setminus \{k\}} \delta_{mk'} \delta_{mk}. \quad (66)$$

The last term can be computed by exploiting the independence of the channel and noise, as follows

$$T_{13} = c_{mk}^2 \mathbb{E}\{|w_{pmk}|^2\} \mathbb{E}\{|u_{mk}|^2\} = c_{mk}^2 \delta_{mk}. \quad (67)$$

By inserting (65)–(67) into (64) and with the aid of some algebraic steps, we obtain

$$\mathbb{E}\{|\hat{u}_{mk}^* u_{mk}|^2\} = 2c_{mk}^2 p \tau_p \xi_{mk} + \gamma_{mk}^2 + c_{mk} \sqrt{p \tau_p} \delta_{mk}^2 = 2c_{mk}^2 p \tau_p \xi_{mk} + \gamma_{mk}^2 + \gamma_{mk} \delta_{mk}, \quad (68)$$

where the final identity uses the relationship between γ_{mk} and c_{mk} in (13). Combining (63) and (68), the first term in the denominator of (30) simplifies to

$$\mathbb{E}\{|\text{BU}_k|^2\} = 2\rho_u \eta_k p \tau_p \sum_{m=1}^M c_{mk}^2 \xi_{mk} + \rho_u \eta_k \sum_{m=1}^M \gamma_{mk} \delta_{mk}. \quad (69)$$

The second term in the denominator of (30) can be split into the two terms based on the pilot reuse pattern defined in \mathcal{P}_k , as follows

$$\sum_{k'=1, k' \neq k}^K \mathbb{E}\{|\text{UI}_{k'k}|^2\} = \sum_{k' \notin \mathcal{P}_k} \mathbb{E}\{|\text{UI}_{k'k}|^2\} + \sum_{k' \in \mathcal{P}_k \setminus \{k\}} \mathbb{E}\{|\text{UI}_{k'k}|^2\}. \quad (70)$$

The first term in the right-hand side of (70) is the non-coherent interference, which is equal to

$$\begin{aligned} \sum_{k' \notin \mathcal{P}_k} \mathbb{E}\{|\text{UI}_{k'k}|^2\} &= \rho_u \sum_{k' \notin \mathcal{P}_k} \eta_{k'} \mathbb{E} \left\{ \left| \sum_{m=1}^M \hat{u}_{mk}^* u_{mk'} \right|^2 \right\} = \rho_u \sum_{k' \notin \mathcal{P}_k} \sum_{m=1}^M \eta_{k'} \mathbb{E} \{ |\hat{u}_{mk}^* u_{mk'}|^2 \} \\ &= \rho_u \sum_{k' \notin \mathcal{P}_k} \sum_{m=1}^M \eta_{k'} \mathbb{E} \{ |\hat{u}_{mk}|^2 \} \mathbb{E} \{ |u_{mk'}|^2 \} = \rho_u \sum_{k' \notin \mathcal{P}_k} \sum_{m=1}^M \eta_{k'} \gamma_{mk} \delta_{mk'}. \end{aligned} \quad (71)$$

The second term in the right-hand side of (70) is the coherent interference. By using (7) and (11), it simplifies as follows

$$\begin{aligned} \mathbb{E}\{|\text{UI}_{k'k}|^2\} &= \mathbb{E} \left\{ \left| \sum_{m=1}^M c_{mk} y_{pmk}^* u_{mk'} \right|^2 \right\} = \mathbb{E} \left\{ \left| \sum_{m=1}^M c_{mk} \left(\sum_{k'' \in \mathcal{P}_k} \sqrt{p \tau_p} u_{mk''}^* + w_{pmk}^* \right) u_{mk'} \right|^2 \right\} \\ &= \rho_u \eta_{k'} \mathbb{E} \left\{ \left| \sum_{m=1}^M c_{mk} w_{pmk}^* u_{mk'} \right|^2 \right\} + \underbrace{\rho_u \eta_{k'} p \tau_p \mathbb{E} \left\{ \left| \sum_{m=1}^M c_{mk} \left(\sum_{k'' \in \mathcal{P}_k \setminus \{k'\}} u_{mk''}^* \right) u_{mk'} \right|^2 \right\}}_{=T_{21}} \\ &\quad + \underbrace{\rho_u \eta_{k'} p \tau_p \mathbb{E} \left\{ \left| \sum_{m=1}^M c_{mk} |u_{mk'}|^2 \right|^2 \right\}}_{=T_{22}} = \rho_u \eta_{k'} \sum_{m=1}^M c_{mk}^2 \delta_{mk'} + \rho_u \eta_{k'} p \tau_p (T_{21} + T_{22}), \end{aligned} \quad (72)$$

which is obtained by using the identity $\mathbb{E}\{|X + Y|^2\} = \mathbb{E}\{|X|^2\} + \mathbb{E}\{|Y|^2\}$, which holds true for zero-mean and independent random variables. The expectation T_{21} can be simplified as follows

$$T_{21} = \sum_{m=1}^M \sum_{k'' \in \mathcal{P}_k \setminus \{k'\}} c_{mk}^2 \mathbb{E}\{|u_{mk''}|^2\} \mathbb{E}\{|u_{mk'}|^2\} = \sum_{m=1}^M \sum_{k'' \in \mathcal{P}_k \setminus \{k'\}} c_{mk}^2 \delta_{mk''} \delta_{mk'}, \quad (73)$$

Similarly, the expectation T_{22} in (72) can be simplified as follows

$$\begin{aligned} T_{22} &= \sum_{m=1}^M \sum_{m'=1}^M c_{mk} c_{m'k} \mathbb{E}\{|u_{mk'}|^2 |u_{m'k'}|^2\} = \sum_{m=1}^M c_{mk}^2 \mathbb{E}\{|u_{mk'}|^4\} + \sum_{m=1}^M \sum_{m'=1, m' \neq m}^M c_{mk} c_{m'k} \\ &\times \mathbb{E}\{|u_{mk'}|^2 |u_{m'k'}|^2\} = 2 \sum_{m=1}^M c_{mk}^2 \delta_{mk'}^2 + 2 \sum_{m=1}^M c_{mk}^2 \xi_{mk'} + \sum_{m=1}^M \sum_{m'=1, m' \neq m}^M c_{mk} c_{m'k} \delta_{mk'} \delta_{m'k'} \\ &= \sum_{m=1}^M c_{mk}^2 \delta_{mk'}^2 + 2 \sum_{m=1}^M c_{mk}^2 \xi_{mk'} + \left(\sum_{m=1}^M c_{mk} \delta_{mk'} \right)^2. \end{aligned} \quad (74)$$

By inserting (73) and (74) into (72), the mutual interference between the user k' and the user k who share the same pilot sequence can be written as follows

$$\begin{aligned} \mathbb{E}\{|U_{k'k}|^2\} &= 2p\tau_p \rho_u \eta_{k'} \sum_{m=1}^M c_{mk}^2 \xi_{mk'} + p\tau_p \rho_u \eta_{k'} \left(\sum_{m=1}^M c_{mk} \delta_{mk'} \right)^2 + p\tau_p \rho_u \eta_{k'} \sum_{m=1}^M \sum_{k'' \in \mathcal{P}_k} c_{mk}^2 \delta_{mk''} \delta_{mk'} \\ &+ \rho_u \eta_{k'} \sum_{m=1}^M c_{mk}^2 \delta_{mk'} = 2p\tau_p \rho_u \eta_{k'} \sum_{m=1}^M c_{mk}^2 \xi_{mk'} + p\tau_p \rho_u \eta_{k'} \left(\sum_{m=1}^M c_{mk} \delta_{mk'} \right)^2 + \rho_u \eta_{k'} \gamma_{mk} \delta_{mk'}. \end{aligned} \quad (75)$$

Finally, the expectation of the additive noise after MR processing is as follows

$$\mathbb{E}\{|NO_k|^2\} = \sum_{m=1}^M \mathbb{E}\{|\hat{u}_{mk}^* w_{um}|^2\} = \sum_{m=1}^M \mathbb{E}\{|\hat{u}_{mk}|^2\} \mathbb{E}\{|w_{um}|^2\} = \sum_{m=1}^M \gamma_{mk}, \quad (76)$$

thanks to the independence between the channel estimate and the noise. By inserting (62), (64), (75), and (76) into the ergodic SINR in (30) and doing some algebra, we conclude the proof.

E. Proof of Theorem 2

Consider the downlink SINR expression (45). Thanks to the uncorrelation between the channel estimate and the estimation error, the numerator simplifies to

$$|DS_{dk}|^2 = \rho_d \left| \sum_{m=1}^M \sqrt{\eta_{mk}} \mathbb{E}\{|\hat{u}_{mk}|^2\} \right|^2 = \rho_d \left(\sum_{m=1}^M \sqrt{\eta_{mk}} \gamma_{mk} \right)^2. \quad (77)$$

The beamforming uncertainty term in the denominator of (45) can be simplified by using (11), as follows

$$\begin{aligned} \mathbb{E}\{|BU_{dk}|^2\} &= \underbrace{\rho_d \sum_{m=1}^M \eta_{mk} c_{mk}^2 \mathbb{E}\{|u_{mk} y_{pmk}^*|^2\}}_{=T_{d1}} - \rho_d \sum_{m=1}^M \eta_{mk} |\mathbb{E}\{|\hat{u}_{mk}|^2\}|^2 = \rho_d T_{d1} - \rho_d \sum_{m=1}^M \eta_{mk} \gamma_{mk}^2, \end{aligned} \quad (78)$$

where we have used the identities $\mathbb{E}\{|X - \mathbb{E}\{X\}|^2\} = \mathbb{E}\{|X|^2\} - |\mathbb{E}\{X\}|^2$ and $\mathbb{E}\{|X + Y|^2\} = \mathbb{E}\{|X|^2\} + \mathbb{E}\{|Y|^2\}$ for zero-mean uncorrelated random variables. By using the identities in (64) and (68), T_{d1} can be formulated as follows

$$T_{d1} = 2p\tau_p\rho_d \sum_{m=1}^M \eta_{mk}\xi_{mk} + \rho_d \sum_{m=1}^M \eta_{mk}\gamma_{mk}^2 + \rho_d \sum_{m=1}^M \eta_{mk}\gamma_{mk}\delta_{mk}, \quad (79)$$

by using (7). The mutual interference term in the denominator of (45) can be rewritten as follows

$$\sum_{k'=1, k' \neq k}^K \mathbb{E}\{|U_{dk'k}|^2\} = \rho_d \sum_{k' \notin \mathcal{P}_k} \sum_{m=1}^M \eta_{mk'}\delta_{mk'}\gamma_{mk'} + \underbrace{\sum_{k' \in \mathcal{P}_k \setminus \{k\}} \rho_d \mathbb{E}\{|U_{dk'k}|^2\}}_{=T_d}, \quad (80)$$

where the first term in the right-hand side of (80) is obtained by exploiting the orthogonality of the pilot sequences. In the second summation of (80), the $T_d = \mathbb{E}\{|U_{dkk'}|^2\}$ can be rewritten as follows

$$\begin{aligned} T_d &= \rho_d \mathbb{E} \left\{ \left| \sum_{m=1}^M \sqrt{\eta_{mk'}} u_{mk} \hat{u}_{mk'}^* \right|^2 \right\} = \rho_d \mathbb{E} \left\{ \left| \sum_{m=1}^M \sqrt{\eta_{mk'}} c_{mk'} u_{mk} y_{pmk'}^* \right|^2 \right\} \\ &= \rho_d \mathbb{E} \left\{ \left| \sum_{m=1}^M \sqrt{\eta_{mk'}} c_{mk'} u_{mk} \left(\sum_{k'' \in \mathcal{P}_k} \sqrt{p\tau_p} u_{mk''}^* + w_{pmk'}^* \right) \right|^2 \right\} = \rho_d \sum_{m=1}^M \eta_{mk'} c_{mk'}^2 \mathbb{E}\{|u_{mk} w_{pmk'}^*|^2\} \\ &\quad + \underbrace{\rho_d p\tau_p \mathbb{E} \left\{ \left| \sum_{m=1}^M \sqrt{\eta_{mk'}} c_{mk'} u_{mk} \left(\sum_{k'' \in \mathcal{P}_k \setminus \{k\}} u_{mk''}^* \right) \right|^2 \right\}}_{=T_{d21}} + \underbrace{\rho_d p\tau_p \mathbb{E} \left\{ \left| \sum_{m=1}^M \sqrt{\eta_{mk'}} c_{mk'} |u_{mk}|^2 \right|^2 \right\}}_{=T_{d22}} \\ &= \rho_d \sum_{m=1}^M \eta_{mk'} c_{mk'}^2 \delta_{mk} + \rho_d p\tau_p (T_{d21} + T_{d22}), \end{aligned} \quad (81)$$

which is obtained by taking into account that the noise is circularly symmetric. The term T_{d21} depends on the non-coherent interference and can be simplified as follows

$$T_{d21} = \sum_{k'' \in \mathcal{P}_k \setminus \{k\}} \sum_{m=1}^M \eta_{mk'} c_{mk'}^2 \mathbb{E}\{|u_{mk} u_{mk''}^*|^2\} = \sum_{k'' \in \mathcal{P}_k \setminus \{k\}} \sum_{m=1}^M \eta_{mk'} c_{mk'}^2 \delta_{mk} \delta_{mk''}, \quad (82)$$

by using the second moment in (9) and the independence among the aggregated channels. The last term T_{d22} in (81) can be simplified as follows

$$\begin{aligned} T_{d22} &= \sum_{m=1}^M \sum_{m'=1}^M \sqrt{\eta_{mk'} \eta_{m'k'}} c_{mk'} c_{m'k'} \mathbb{E}\{|u_{mk}|^2 |u_{m'k}|^2\} = \sum_{m=1}^M \eta_{mk'} c_{mk'}^2 \mathbb{E}\{|u_{mk}|^4\} \\ &\quad + \sum_{m=1}^M \sum_{m'=1, m' \neq m}^M \sqrt{\eta_{mk'} \eta_{m'k'}} c_{mk'} c_{m'k'} \mathbb{E}\{|u_{mk}|^2\} \mathbb{E}\{|u_{m'k}|^2\} \end{aligned} \quad (83)$$

$$= \sum_{m=1}^M \eta_{mk'} c_{mk'}^2 \delta_{mk}^2 + 2 \sum_{m=1}^M \eta_{mk'} c_{mk'}^2 \xi_{mk} + \left(\sum_{m=1}^M \sqrt{\eta_{mk'}} c_{mk'} \xi_{mk} \right)^2,$$

where the last equality follows from Lemma 1. By inserting (82) and (83) into (81), (80) can be rewritten as follows

$$\begin{aligned} \sum_{k'=1, k' \neq k}^K \mathbb{E}\{|U_{dk'k}|^2\} &= \rho_d \sum_{k'=1, k' \neq k}^K \sum_{m=1}^M \eta_{mk'} \delta_{mk} \gamma_{mk'} \\ &+ \rho_d p \tau_p \sum_{k' \in \mathcal{P}_k \setminus \{k\}} \left(\sum_{m=1}^M \sqrt{\eta_{mk'}} c_{mk'} \delta_{mk} \right)^2 + 2 \rho_d p \tau_p \sum_{k' \in \mathcal{P}_k \setminus \{k\}} \sum_{m=1}^M \eta_{mk'} c_{mk'}^2 \xi_{mk}, \end{aligned} \quad (84)$$

Finally, plugging (77), (78), and (84) into (45) and using some algebra, the proof follows.

REFERENCES

- [1] T. V. Chien, H. Q. Ngo, S. Chatzinotas, M. D. Renzo, and B. Ottersten, “RIS and Cell-Free Massive MIMO: A marriage for harsh propagation environments,” in *Proc. IEEE GLOBECOM*, 2021, will be submitted.
- [2] M. Giordani, M. Polese, M. Mezzavilla, S. Rangan, and M. Zorzi, “Toward 6G networks: Use cases and technologies,” *IEEE Commun. Mag.*, vol. 58, no. 3, pp. 55–61, 2020.
- [3] T. V. Chien and E. Björnson, *Massive MIMO Communications*. Springer International Publishing, 2017, pp. 77–116.
- [4] T. S. Rappaport, Y. Xing, G. R. MacCartney, A. F. Molisch, E. Mellios, and J. Zhang, “Overview of millimeter wave communications for fifth-generation (5G) wireless networks—With a focus on propagation models,” *IEEE Trans. Antennas Propag.*, vol. 65, no. 12, pp. 6213–6230, 2017.
- [5] E. Björnson, L. Sanguinetti, and M. Kountouris, “Deploying dense networks for maximal energy efficiency: Small cells meet massive MIMO,” *IEEE J. Sel. Areas Commun.*, vol. 34, no. 4, pp. 832–847, 2016.
- [6] T. Van Chien, T. N. Canh, E. Björnson, and E. G. Larsson, “Power control in cellular massive MIMO with varying user activity: A deep learning solution,” *IEEE Transactions on Wireless Communications*, 2020.
- [7] H. Q. Ngo, A. Ashikhmin, H. Yang, E. G. Larsson, and T. L. Marzetta, “Cell-free massive MIMO versus small cells,” *IEEE Trans. Wireless Commun.*, vol. 16, no. 3, pp. 1834–1850, 2017.
- [8] T. Van Chien, E. Björnson, and E. G. Larsson, “Joint power allocation and load balancing optimization for energy-efficient cell-free Massive MIMO networks,” *IEEE Trans. Wireless Commun.*, vol. 19, no. 10, pp. 6798–6812, 2020.
- [9] E. Björnson and L. Sanguinetti, “Scalable cell-free massive MIMO systems,” *IEEE Trans. Commun.*, vol. 68, no. 7, pp. 4247–4261, 2020.
- [10] Q. Wu and R. Zhang, “Intelligent reflecting surface enhanced wireless network via joint active and passive beamforming,” *IEEE Trans. Wireless Commun.*, vol. 18, no. 11, pp. 5394–5409, 2019.
- [11] T. A. Le, T. Van Chien, and M. Di Renzo, “Robust probabilistic-constrained optimization for IRS-aided MISO communication systems,” *IEEE Wireless Commun. Lett.*, 2020.
- [12] M. Di Renzo, A. Zappone, M. Debbah, M. S. Alouini, C. Yuen, J. de Rosny, and S. Tretyakov, “Smart radio environments empowered by reconfigurable intelligent surfaces: How it works, state of research, and the road ahead,” *IEEE J. Sel. Areas Commun.*, vol. 38, no. 11, pp. 2450–2525, 2020.
- [13] Q. Wu, S. Zhang, B. Zheng, C. You, and R. Zhang, “Intelligent reflecting surface aided wireless communications: A tutorial,” *IEEE Trans. Commun.*, pp. 1–1, 2021.
- [14] M. M. Zhao, Q. Wu, M. J. Zhao, and R. Zhang, “Intelligent reflecting surface enhanced wireless networks: Two-timescale beamforming optimization,” *IEEE Trans. Wireless Commun.*, vol. 20, no. 1, pp. 2–17, 2021.
- [15] A. Zappone, M. Di Renzo, F. Shams, X. Qian, and M. Debbah, “Overhead-aware design of reconfigurable intelligent surfaces in smart radio environments,” *IEEE Trans. Wireless Commun.*, vol. 20, no. 1, pp. 126–141, 2021.

- [16] A. Abrardo, D. Dardari, and M. Di Renzo, "Intelligent reflecting surfaces: Sum-rate optimization based on statistical CSI," *arXiv preprint arXiv:2012.10679*, 2020.
- [17] B. Zheng and R. Zhang, "Intelligent reflecting surface-enhanced OFDM: Channel estimation and reflection optimization," *IEEE Wireless Commun. Lett.*, vol. 9, no. 4, pp. 518–522, 2020.
- [18] X. Wei, D. Shen, and L. Dai, "Channel estimation for RIS assisted wireless communications: Part I-Fundamentals, solutions, and future opportunities," *IEEE Commun. Lett.*, 2021.
- [19] N. S. Perović, L.-N. Tran, M. Di Renzo, and M. F. Flanagan, "Achievable rate optimization for MIMO systems with reconfigurable intelligent surfaces," *IEEE Trans. Wireless Commun.*, 2021.
- [20] T. Zhou, K. Xu, X. Xia, W. Xie, and J. Xu, "Achievable rate optimization for aerial intelligent reflecting surface-aided Cell-Free Massive MIMO system," *IEEE Access*, 2020.
- [21] Z. Zhang and L. Dai, "Capacity improvement in wideband reconfigurable intelligent surface-aided cell-free network," in *Proc. IEEE SPAWC*, 2020, pp. 1–5.
- [22] M. Bashar, K. Cumanan, A. G. Burr, P. Xiao, and M. Di Renzo, "On the performance of reconfigurable intelligent surface-aided cell-free massive mimo uplink," in *Proc. IEEE GLOBECOM*, 2020, pp. 1–6.
- [23] Y. Zhang, B. Di, H. Zhang, J. Lin, Y. Li, and L. Song, "Reconfigurable intelligent surface aided cell-free MIMO communications," *IEEE Wireless Commun. Lett.*, pp. 1–1, 2020, accepted for publication.
- [24] Y. Zhang, B. Di, H. Zhang, J. Lin, C. Xu, D. Zhang, Y. Li, and L. Song, "Beyond cell-free MIMO: Energy efficient reconfigurable intelligent surface aided cell-free MIMO communications," *IEEE Trans. on Cog. Comm. and Net.*, 2021.
- [25] T. Van Chien, L. T. Tu, S. Chatzinotas, and B. Ottersten, "Coverage probability and ergodic capacity of intelligent reflecting surface-enhanced communication systems," *IEEE Commun. Lett.*, vol. 25, no. 1, pp. 69–73, 2021.
- [26] T. Hou, Y. Liu, Z. Song, X. Sun, Y. Chen, and L. Hanzo, "Reconfigurable intelligent surface aided NOMA networks," *IEEE J. Sel. Areas Commun.*, vol. 38, no. 11, pp. 2575–2588, 2020.
- [27] T. Van Chien, A. K. Papazafeiropoulos, L. T. Tu, R. Chopra, S. Chatzinotas, and B. Ottersten, "Outage probability analysis of IRS-assisted systems under spatially correlated channels," *arXiv preprint arXiv:2102.11408*, 2021.
- [28] M. Di Renzo, M. Debbah, D.-T. Phan-Huy, A. Zappone, M.-S. Alouini, C. Yuen, V. Sciancalepore, G. C. Alexandropoulos, J. Hoydis, H. Gacanin *et al.*, "Smart radio environments empowered by reconfigurable AI meta-surfaces: An idea whose time has come," *EURASIP Journal on Wireless Communications and Networking*, vol. 2019, no. 1, pp. 1–20, 2019.
- [29] H. Alwazani, A. Kammoun, A. Chaaban, M. Debbah, and M.-S. Alouini, "Intelligent reflecting surface-assisted multi-user MISO communication: Channel estimation and beamforming design," *IEEE Open Jour. of the Commun. Soc.*, vol. 1, pp. 661–680, 2020.
- [30] E. Björnson and L. Sanguinetti, "Rayleigh fading modeling and channel hardening for reconfigurable intelligent surfaces," *IEEE Wireless Commun. Lett.*, 2020.
- [31] S. Kay, *Fundamentals of Statistical Signal Processing: Estimation Theory*. Prentice Hall, 1993.
- [32] T. C. Mai, H. Q. Ngo, M. Egan, and T. Q. Duong, "Pilot power control for Cell-Free Massive MIMO," *IEEE Trans. Veh. Technol.*, vol. 67, no. 11, pp. 11 264–11 268, 2018.
- [33] T. Van Chien, E. Björnson, and E. G. Larsson, "Joint pilot design and uplink power allocation in multi-cell Massive MIMO systems," *IEEE Trans. Wireless Commun.*, vol. 17, no. 3, pp. 2000–2015, 2018.
- [34] H. Cramér, *Random variables and probability distributions*. Cambridge University Press, 2004, vol. 36.
- [35] T. L. Marzetta, E. G. Larsson, H. Yang, and H. Q. Ngo, *Fundamentals of Massive MIMO*. Cambridge University Press, 2016.
- [36] G. Gradoni and M. Di Renzo, "End-to-end mutual coupling aware communication model for reconfigurable intelligent surfaces: An electromagnetic-compliant approach based on mutual impedances," *IEEE Wireless Commun. Lett.*, 2021.
- [37] X. Qian and M. Di Renzo, "Mutual coupling and unit cell aware optimization for reconfigurable intelligent surfaces," *IEEE Wireless Commun. Lett.*, 2021.
- [38] E. Björnson, J. Hoydis, and L. Sanguinetti, "Massive MIMO networks: Spectral, energy, and hardware efficiency," *Foundations and Trends® in Signal Processing*, vol. 11, no. 3-4, pp. 154–655, 2017.
- [39] T. V. Chien and H. Q. Ngo, *Massive MIMO Channels*. IET Publishers, 2020, ch. 11.